

Isolated BHs

Early works

«Halos around black holes» Soviet Astronomy – Astronom. Zhurn (1971)

In this paper accretion onto isolated BHs from the ISM was studied for different BH masses (including intermediate).

Dynamics of accretion, the role of turbulence, the role of magnetic fields in the ISM, spectrum.

Synchrotron radiation of magnetized plasma, which is heated during accretion up to 10^{12} K (here the temperature means the average energy of electrons motion perpendicular to magnetic field lines).

(Development of this approach see in [astro-ph/0403649](https://arxiv.org/abs/astro-ph/0403649))



Victorij Shvartsman

Basic formulae

$$\begin{aligned}\dot{M} &\sim \pi r_{\text{cap}}^2 \rho_{\text{gas}} V \\ &\approx 7.4 \times 10^{13} \text{ g s}^{-1} \left(\frac{M}{M_{\odot}} \right)^2 \left(\frac{n_{\text{gas}}}{10^2 \text{ cm}^{-3}} \right) \left(\frac{V}{10 \text{ km s}^{-1}} \right)^{-3} \\ &\approx 5.3 \times 10^{-4} \dot{M}_{\text{Edd}} \left(\frac{M}{M_{\odot}} \right) \left(\frac{n_{\text{gas}}}{10^2 \text{ cm}^{-3}} \right) \left(\frac{V}{10 \text{ km s}^{-1}} \right)^{-3}\end{aligned}$$

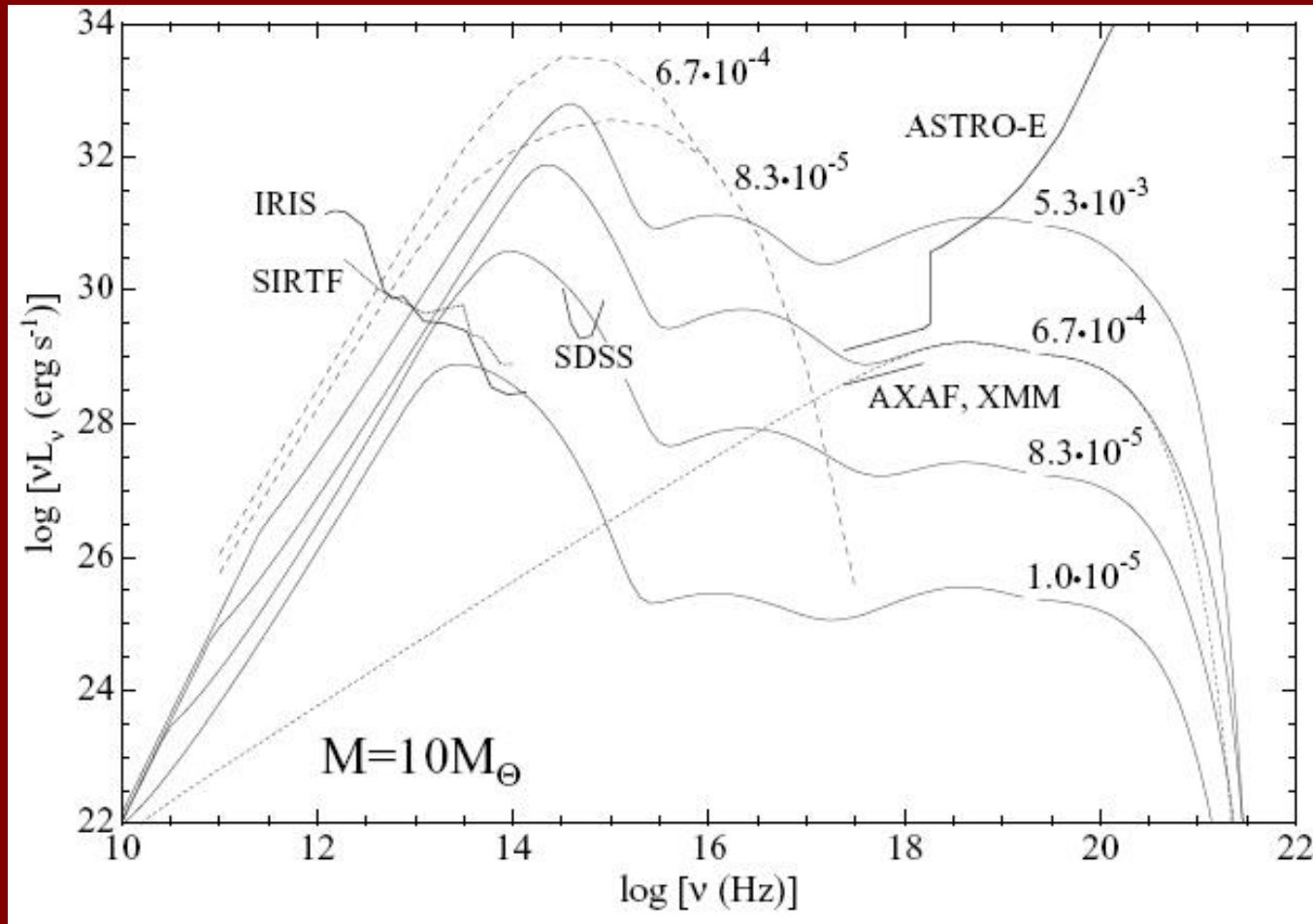
$$v_{\text{turb}} \sim 1.1 (r/1\text{pc})^{0.38} \text{ km s}^{-1},$$

Velocity of turbulent motions

$$V \lesssim 52 (r_g/r_{\text{ofl}})^{0.18} (M/M_{\odot})^{0.14} \text{ km s}^{-1}$$

The critical velocity corresponding to an accretion disc formation.

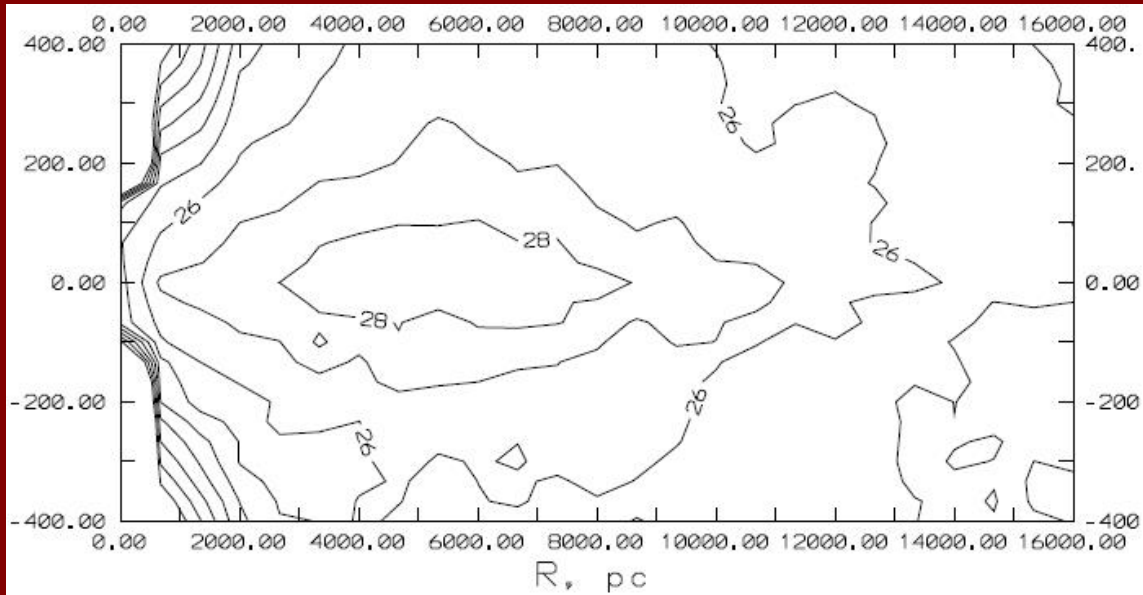
Isolated accreting BHs



ADAF
10 solar masses

The objects mostly
emit in X-rays or IR.

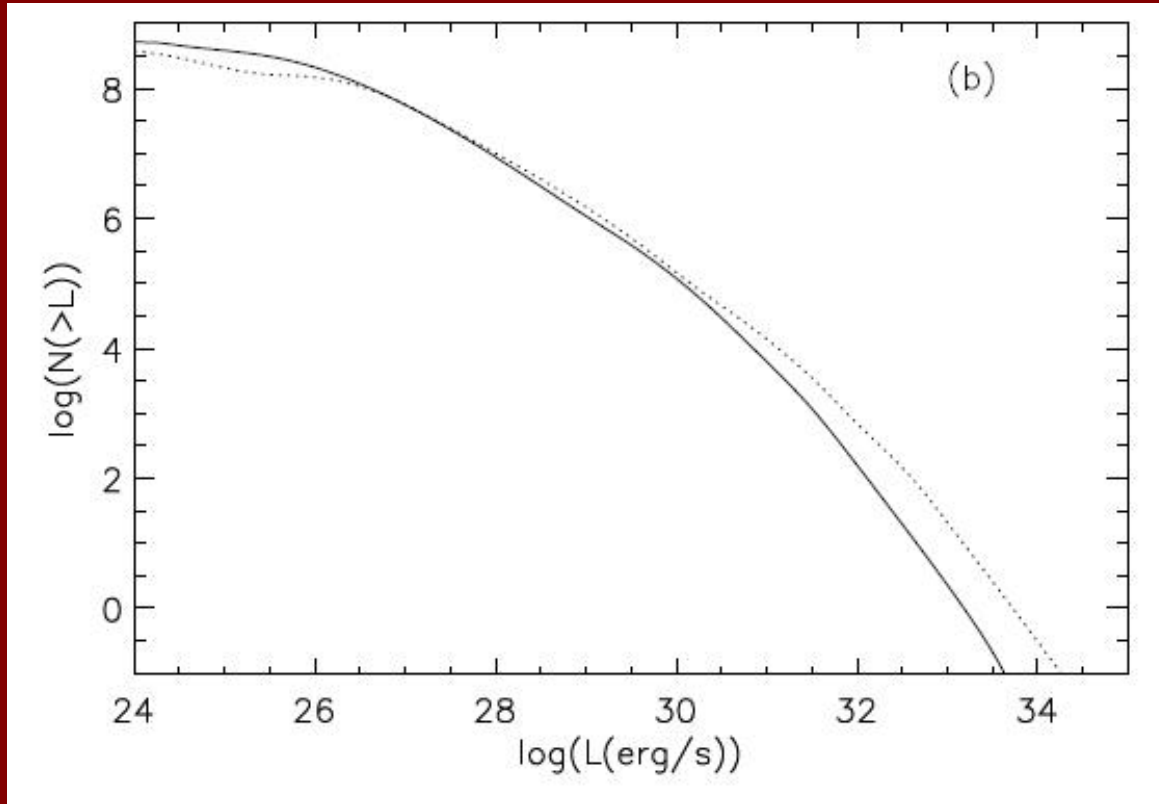
The galactic population of accreting isolated BHs



The luminosity distribution is mostly determined by the ISM distribution, then – by the galactic potential.

It is important that maxima of the ISM distribution and distribution of compact objects roughly coincide. This results in relatively sharp maximum in the luminosity distribution.

Searching in deep surveys



Agol, Kamionkowski (astro-ph/0109539) demonstrated that satellites like XMM or Chandra can discover about few dozens of such sources.

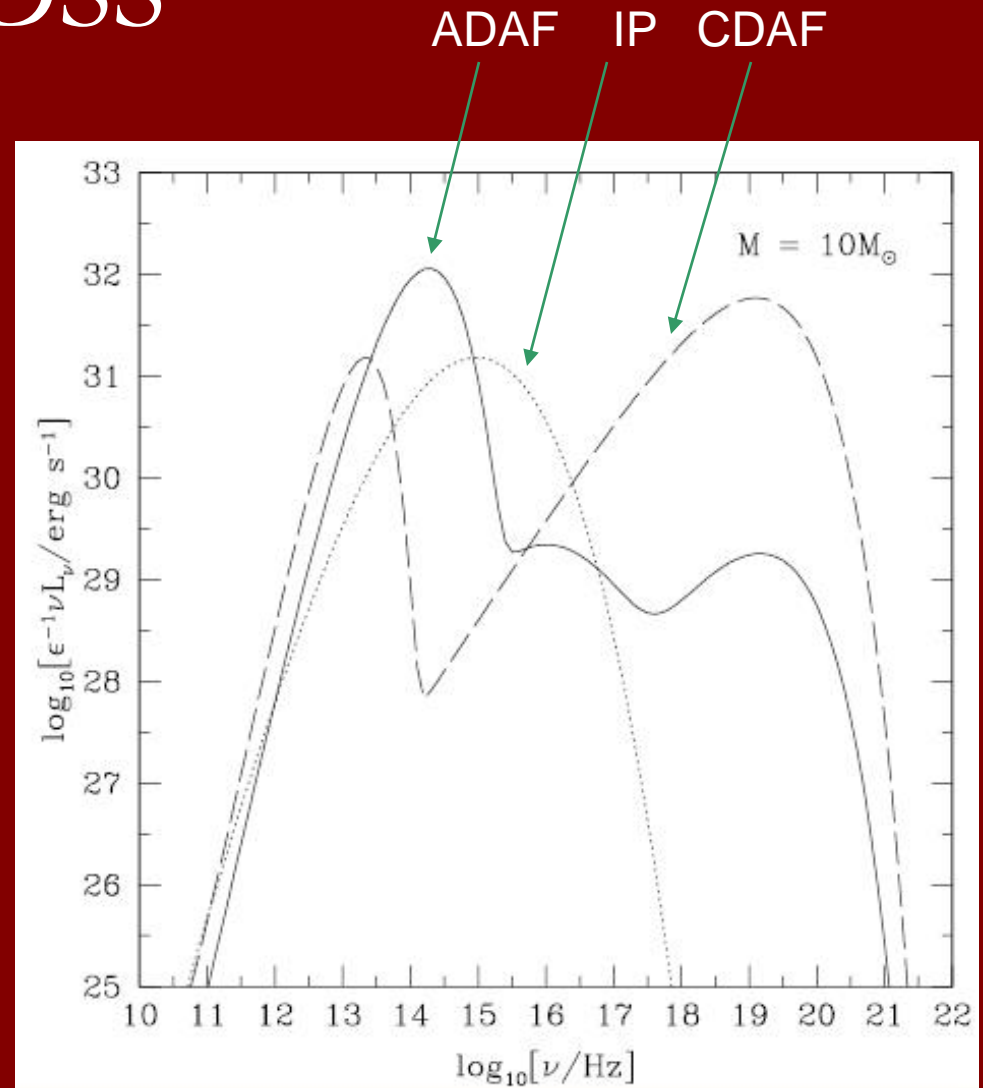
However, it is very difficult to identify isolated accreting BHs.

Digging in the SDSS

The idea is that the synchrotron emission can appear in the optical range and in X-rays.

Cross-correlation between SDSS and ROSAT data resulted in 57 candidates.

Regime of accretion and its efficiency are poorly known



Radio emission from isolated BHs

$$L_R \sim L_X^{0.7}$$

The task for LOFAR?

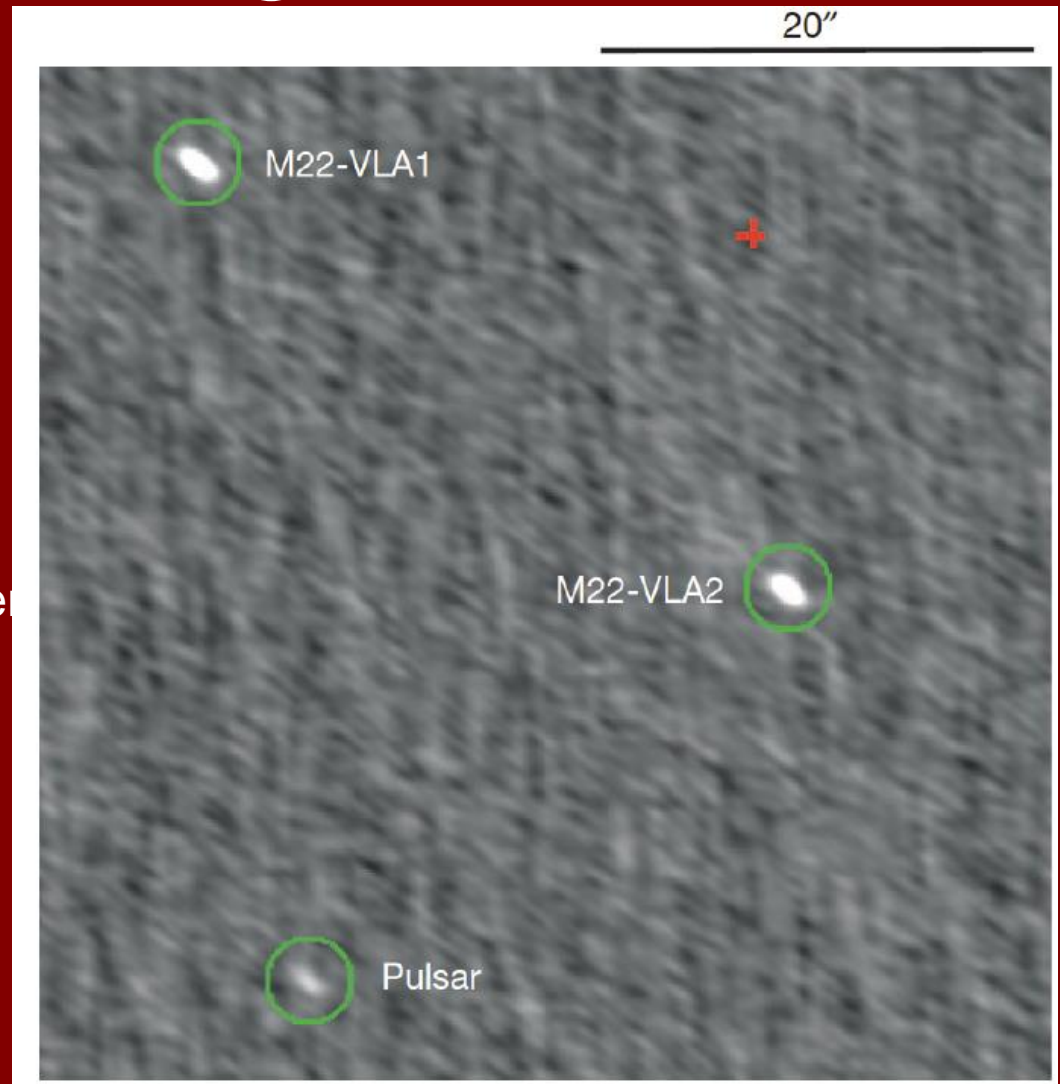
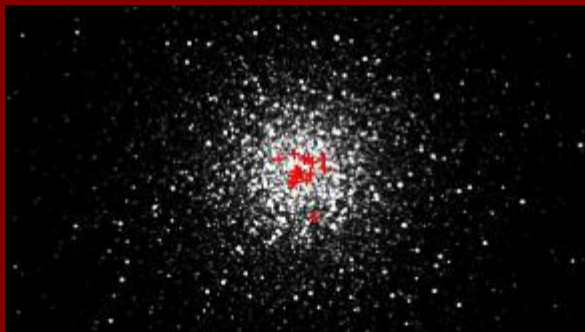
Phase/type	M_{BH}	n_H	T_{ISM}	N_{BH}	L_X	d_{radio}	N_{radio}
GMC Core	10	10^5	10^4	~ 1	5×10^{33}	12	~ 1
GMC/cold neutral	10	10^3	10^4	1.3×10^6	5×10^{29}	0.7	400
warm ISM	10	0.4	10^4	5×10^7	7×10^{22}	.005	0
hot ISM	10	0.01	10^6	5×10^7	5×10^{13}	10^{-5}	0
GMC/cold, fast halo IMBH	2600	10^3	10^4	30	8×10^{30}	15	10
IMBH/disk pop/cold ISM	260	10^3	10^4	*	8×10^{33}	40	*
IMBH/disk pop/GMC	260	10^5	10^4	*	8×10^{37}	800	*
IMBH/disk pop/warm ISM	260	0.4	10^4	*	1×10^{27}	0.5	*

Two isolated BHs in a globular cluster?

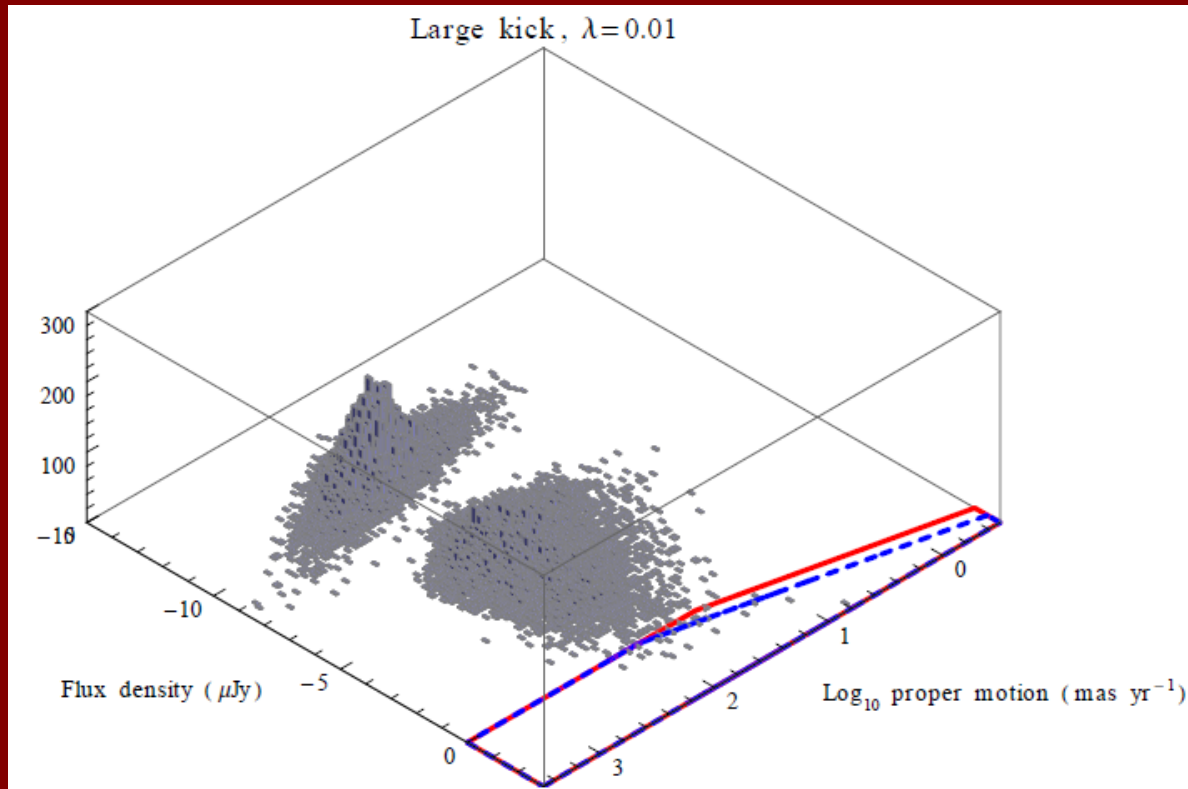
eVLA observations showed two flat-spectrum sources without X-ray or/and optical identifications.

Most probably, they are accreting BHs. Probably, isolated.

Numerical model for the cluster evolution and the number of BHs was calculated in the paper 1211.6608.



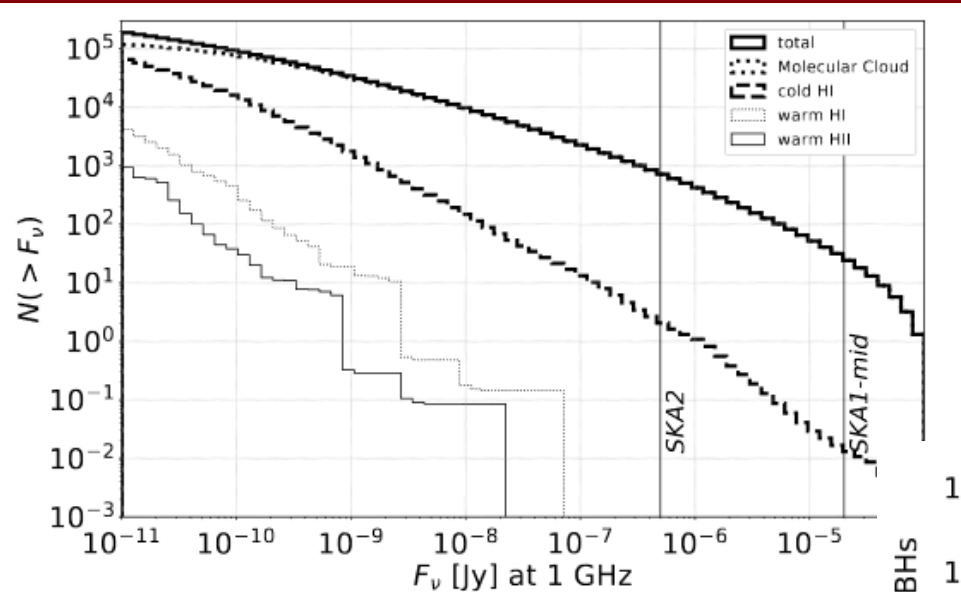
More calculations for radio IBHs



The authors calculate if IBHs can be detected by SKA and other future survey if the accrete from the ISM. Different assumptions about initial velocities and accretion efficiency are made.

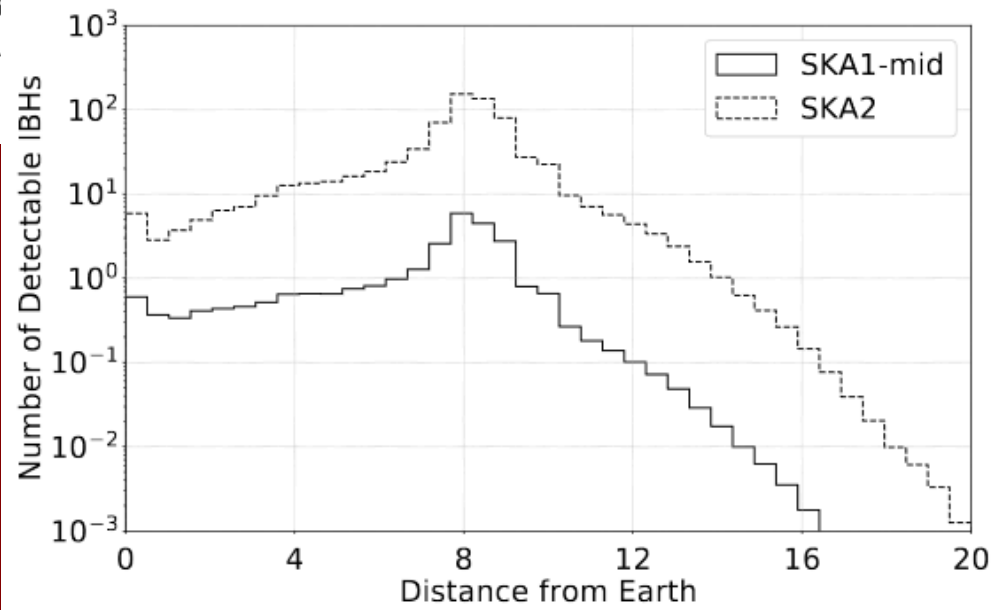
SKA will be effective in discovering isolated accreting BHs due to their radio emission.

Calculations for SKA



Better look at the Galactic center region

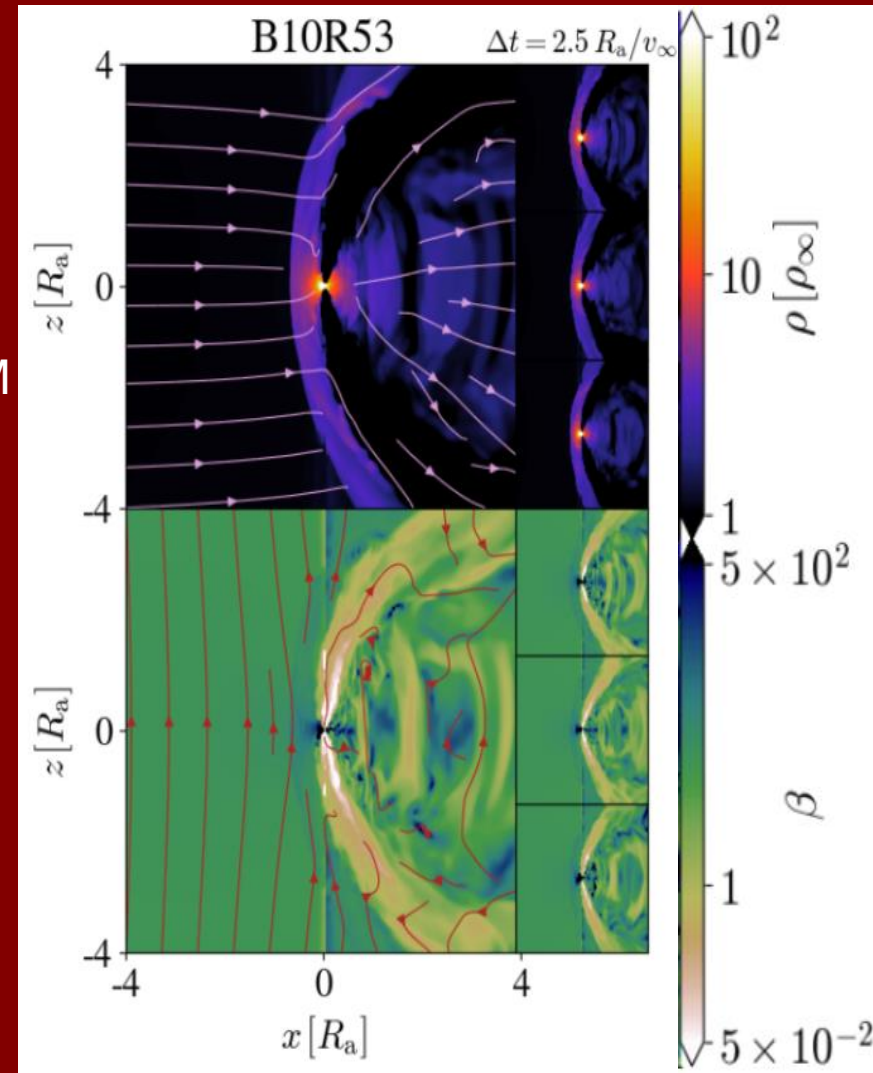
~30 IBHs in SKA-1-mid
~700 IBHs in SKA-2



Jet Formation in Bondi-Hoyle-Lyttleton Accretion

Magnetically arrested disc.
Rapidly rotating BH.

β — ratio of gas to magnetic pressure in ISM
For large β jets are not formed.



Electron-positron jets from isolated BHs

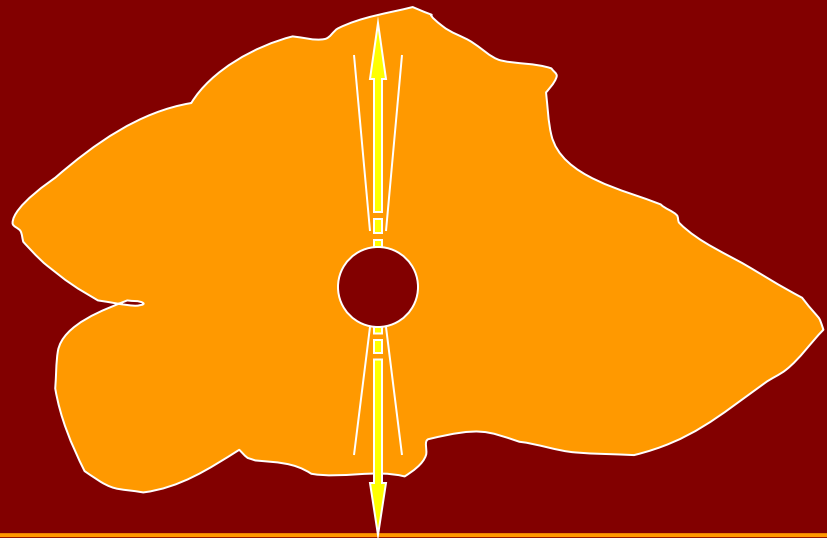
The magnetic flux, accumulated on the horizon of an IBH because of accretion of interstellar matter, allows the Blandford–Znajek mechanism to be activated.

So, electron–positron jets can be launched.

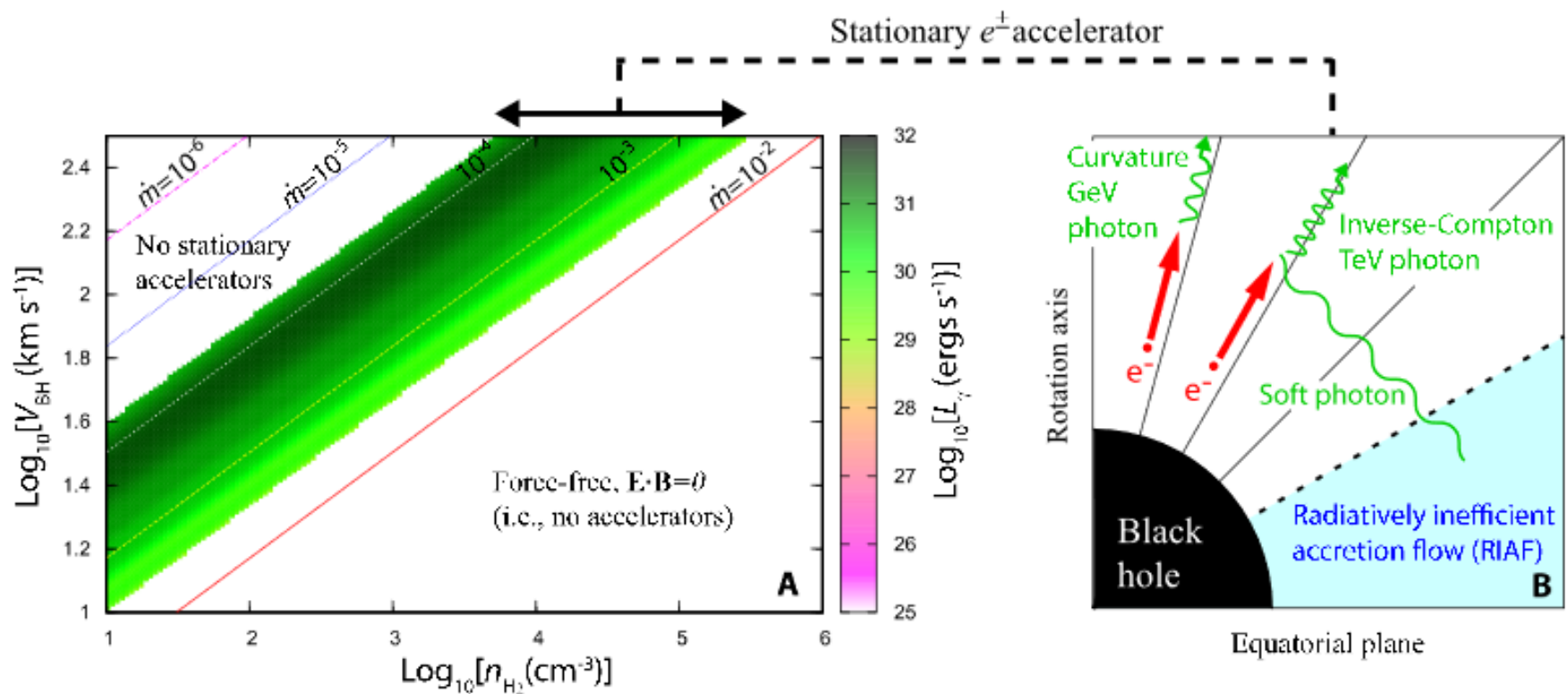
Such jets are feasible electron accelerator which, in molecular clouds, allows electron energy to be boosted up to ~ 1 PeV.

These sources can contribute both to the population of unidentified point-like sources and to the local cosmic-ray electron spectrum.

The inverse Compton emission of these locally generated cosmic rays may explain the variety of gamma-ray spectra detected from nearby molecular clouds.



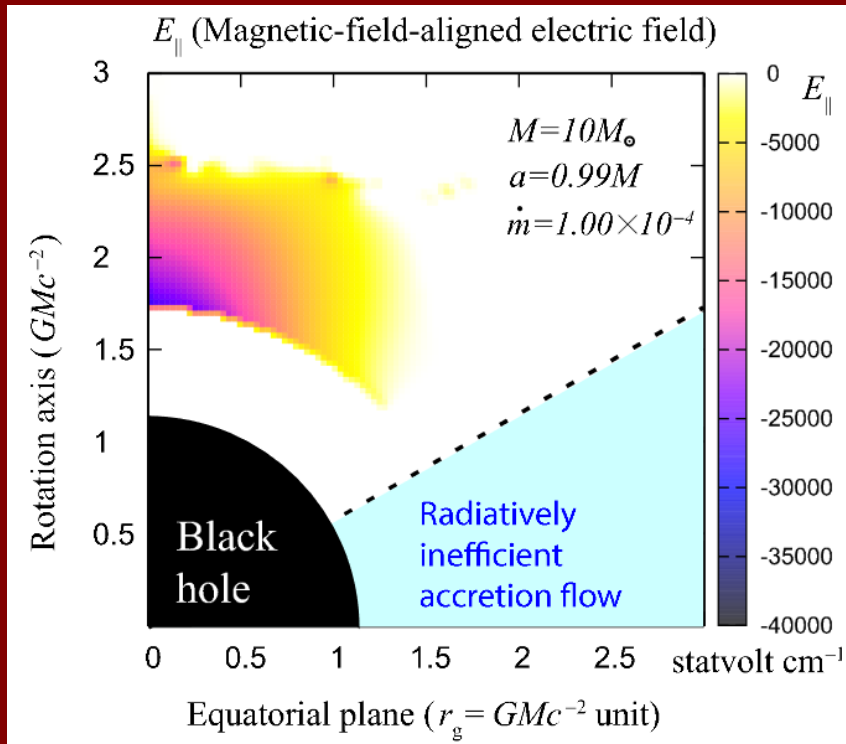
IBHs in molecular clouds as TeV sources



Rotation is important!

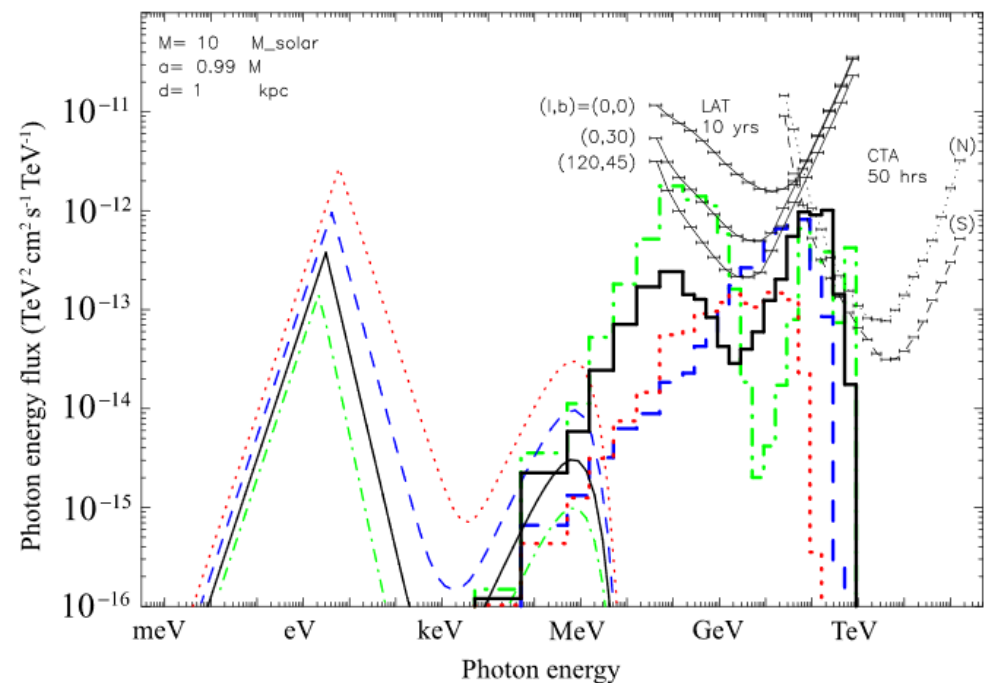
The black holes rotational energy is electromagnetically extracted via the Blandford-Znajek process.

Particle acceleration by rotating IBHs



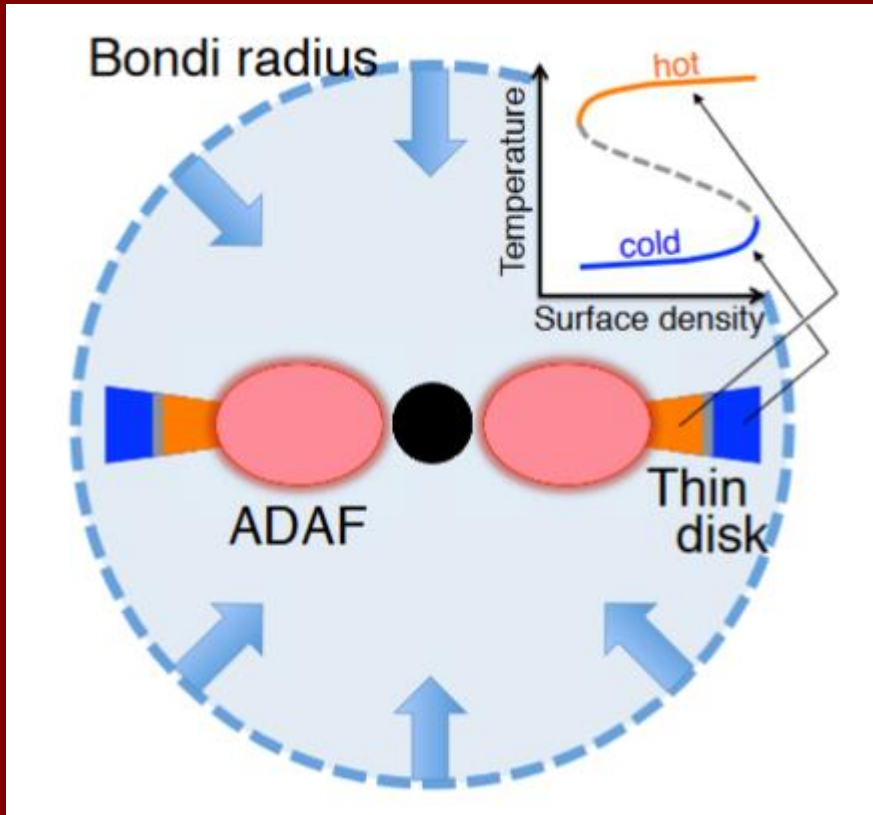
The red dotted, blue dashed, black solid, and green dash-dotted curves correspond to the dimensionless accretion rate of $10^{-3.5}$, $10^{-3.75}$, 10^{-4} , and $10^{-4.25}$, respectively.

The distance is assumed to be 1 kpc.



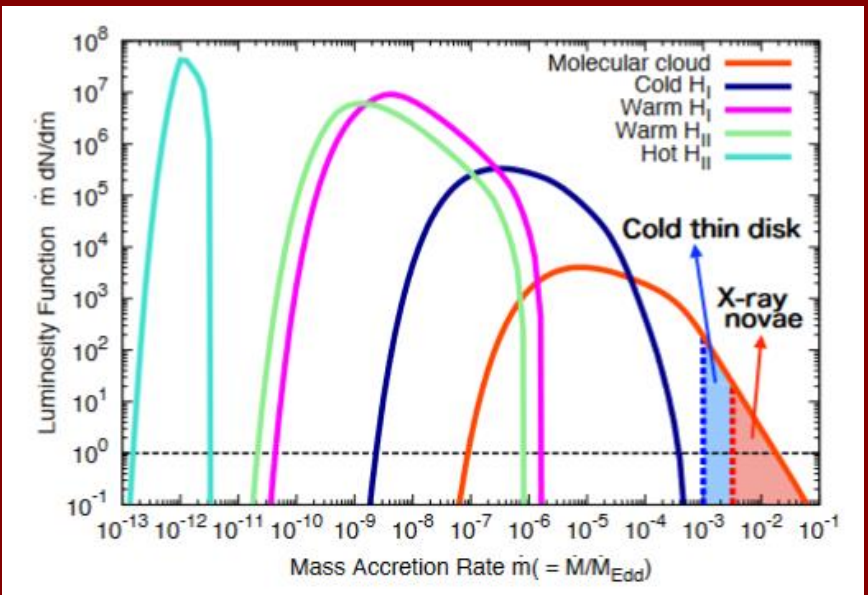
The thin curves on the left denote the input spectra of the ADAF. Such soft photons illuminate the accelerator in the polar funnel. The thick lines denote the spectra of the gamma-rays emitted from the accelerator.

X-ray nova and accreting isolated BHs



Up to several event per year.
Then some of known X-ray nova
with unidentified companions,
can be due to isolated BHs.

Around accreting isolated BHs
in molecular clouds it is possible
to have conditions
(hydrogen-ionization disk instability)
necessary for X-ray nova appearance.



Detailed study of AIBHs

$$\dot{M} = \lambda \cdot 4\pi \frac{(GM)^2 \rho}{(v^2 + c_s^2)^{3/2}}$$

$$\approx 3.7 \times 10^{15} \text{ g s}^{-1}$$

$$\cdot \left(\frac{\lambda}{0.1} \right) \left(\frac{M}{10 \text{ M}_\odot} \right)^2 \left(\frac{\rho}{10^3 \text{ cm}^{-3} m_p} \right) \left[\frac{v^2 + c_s^2}{(10 \text{ km s}^{-1})^2} \right]^{-3/2}$$

$$\eta = \begin{cases} \eta_{\text{std}} (\dot{M} / \dot{M}_{\text{th}}) & (\text{when } \dot{M} < \dot{M}_{\text{th}}) \\ \eta_{\text{std}} & (\text{when } \dot{M}_{\text{th}} < \dot{M} < 2\dot{M}_{\text{Edd}}). \end{cases}$$

RIAF (radiatively-inefficient accretion flow).
Below some threshold the luminosity is reduced.

$$L = \eta \dot{M} c^2$$

$$= 3.4 \times 10^{37} \text{ erg s}^{-1}$$

$$\cdot \eta \lambda \left(\frac{M}{10 \text{ M}_\odot} \right)^2 \left(\frac{\rho}{10^3 \text{ cm}^{-3} m_p} \right) \left[\frac{v^2 + c_s^2}{(10 \text{ km s}^{-1})^2} \right]^{-3/2}$$

Most of AIBHs
are in the RIAF state.

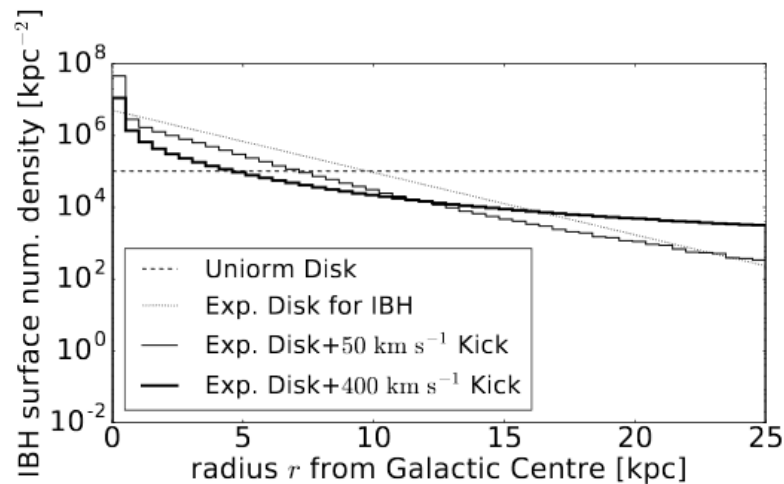
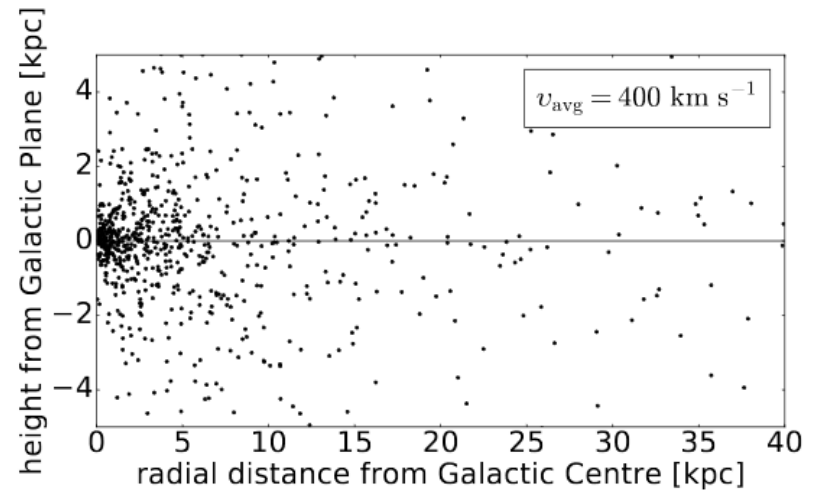
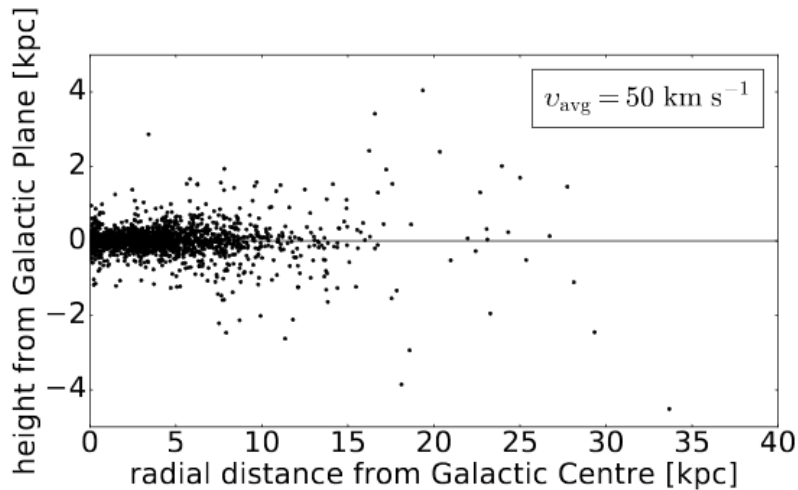
$L = 9.0 \times 10^{32} \text{ erg s}^{-1}$ **RIAF**

$$\cdot \left(\frac{\lambda}{0.1} \right)^2 \left(\frac{M}{10 \text{ M}_\odot} \right)^3 \left(\frac{\rho}{10^3 \text{ cm}^{-3} m_p} \right)^2 \left[\frac{v^2 + c_s^2}{(10 \text{ km s}^{-1})^2} \right]^{-3}$$

$L = 3.4 \times 10^{35} \text{ erg s}^{-1}$ **Standard**

$$\cdot \left(\frac{\lambda}{0.1} \right) \left(\frac{M}{10 \text{ M}_\odot} \right)^2 \left(\frac{\rho}{10^3 \text{ cm}^{-3} m_p} \right) \left[\frac{v^2 + c_s^2}{(10 \text{ km s}^{-1})^2} \right]^{-3/2}$$

Spatial distribution

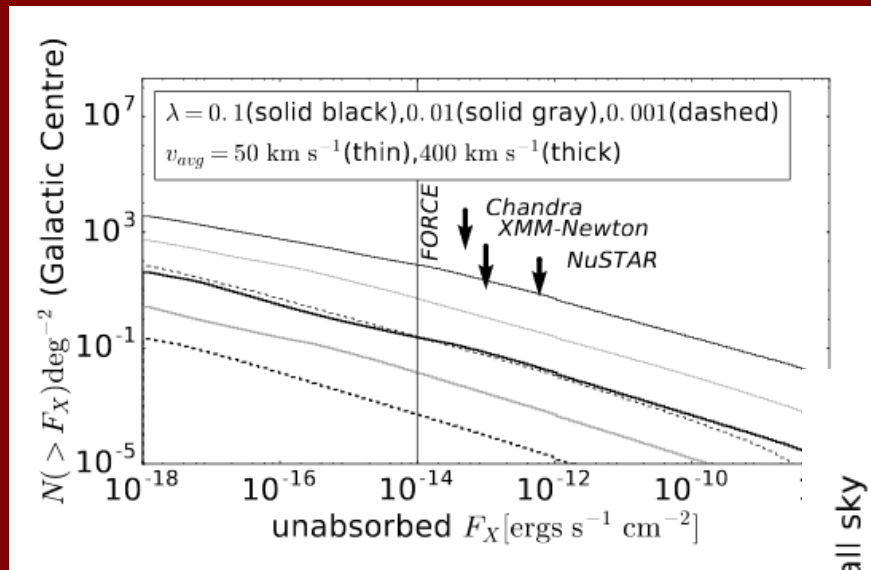


Many BHs leave the Galaxy
for average velocity $>200 \text{ km/s}$

Observability

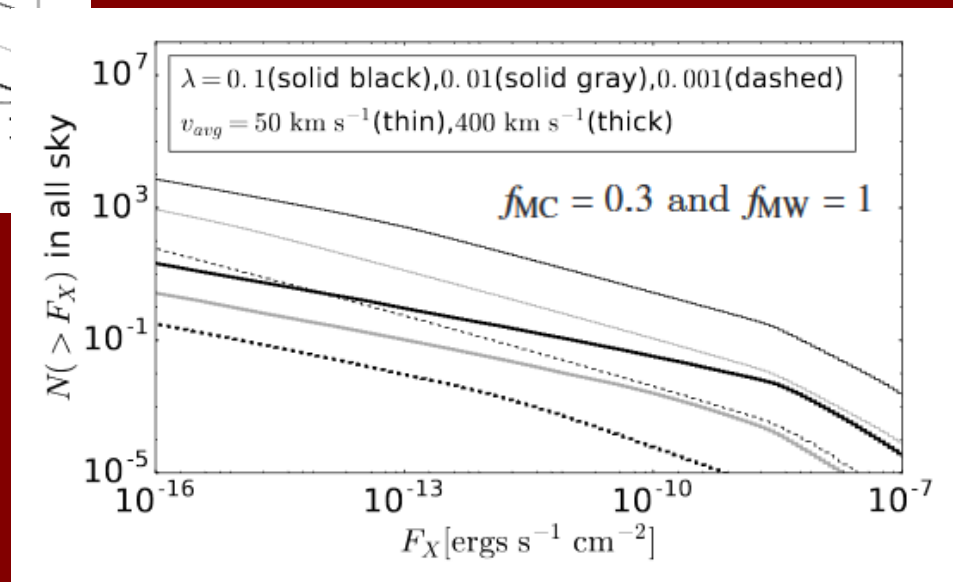
$$dF_{\text{ph}}/d\epsilon_{\text{ph}} \propto \epsilon_{\text{ph}}^{-\zeta}$$

Power-law spectrum in the RIAF regime (hard state)

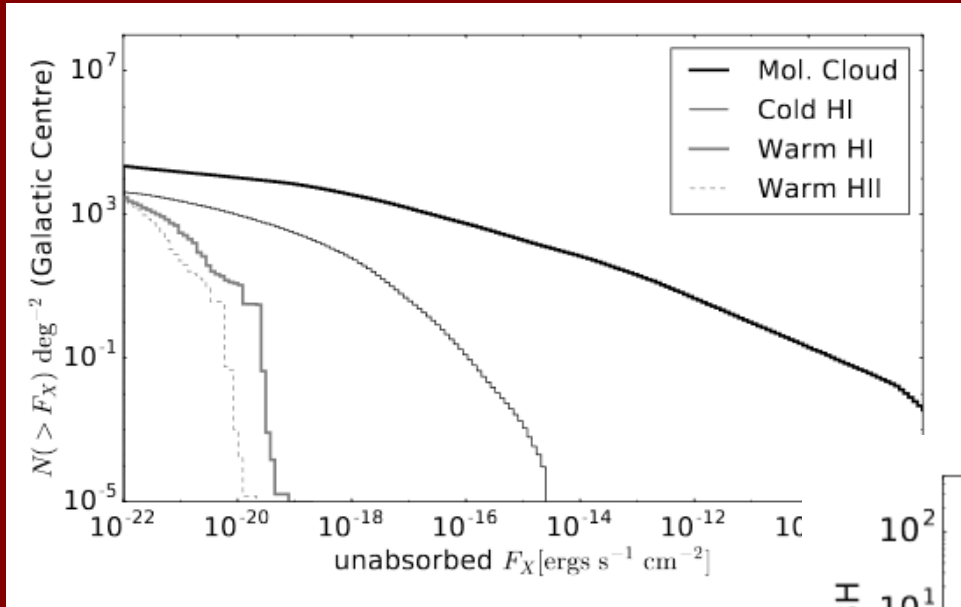


	$v_{\text{avg}} [\text{km s}^{-1}]$				
	50	100	200	300	400
bulge	0.018	1.4×10^{-3}	0.067	3.7×10^{-3}	9.1×10^{-3}
disc	32	4.5	0.79	0.19	0.086

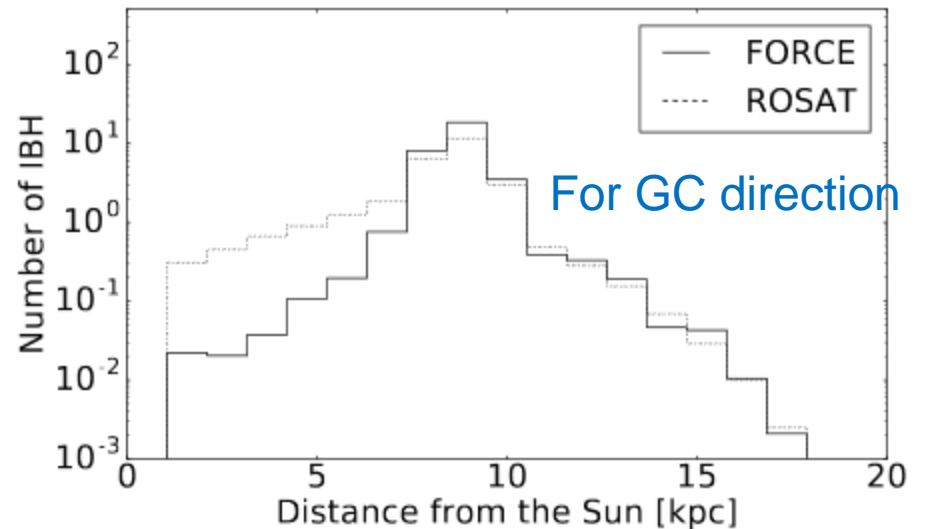
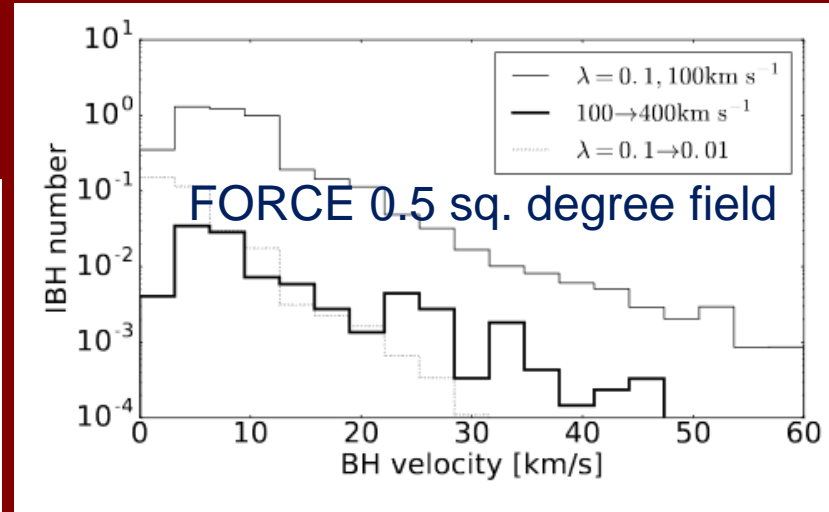
The authors focus on harder X-ray emission than in ROSAT case



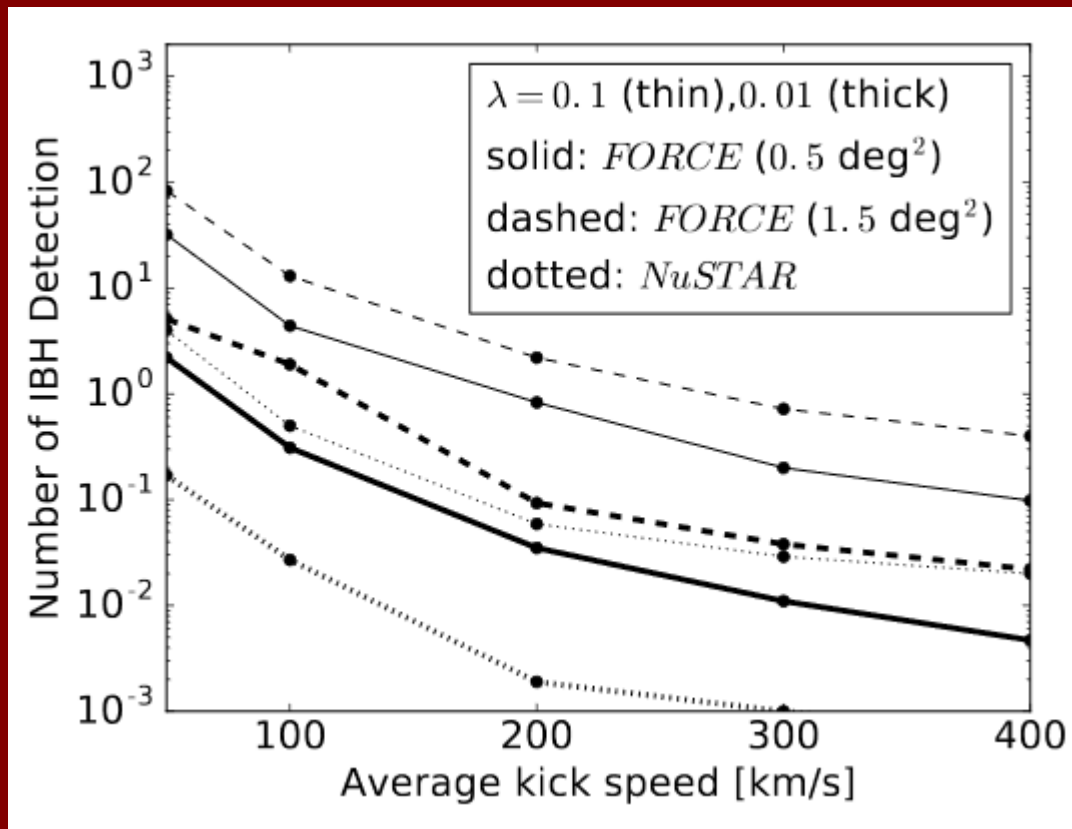
Properties of AIBHs



AIBHs from dense ISM regions contribute more.



Deep survey towards the Galactic center



FORCE is a japanies project,
if approved – then to be launched in mid 2020s.

Magnetically arrested discs

$$V_R \approx \frac{1}{2} \alpha V_K \simeq 1.5 \times 10^9 \mathcal{R}_1^{-1/2} \alpha_{-0.5} \text{ cm s}^{-1},$$

$$k_B T_p \approx \frac{GMm_p}{4R} \simeq 23 \mathcal{R}_1^{-1} \text{ MeV}$$

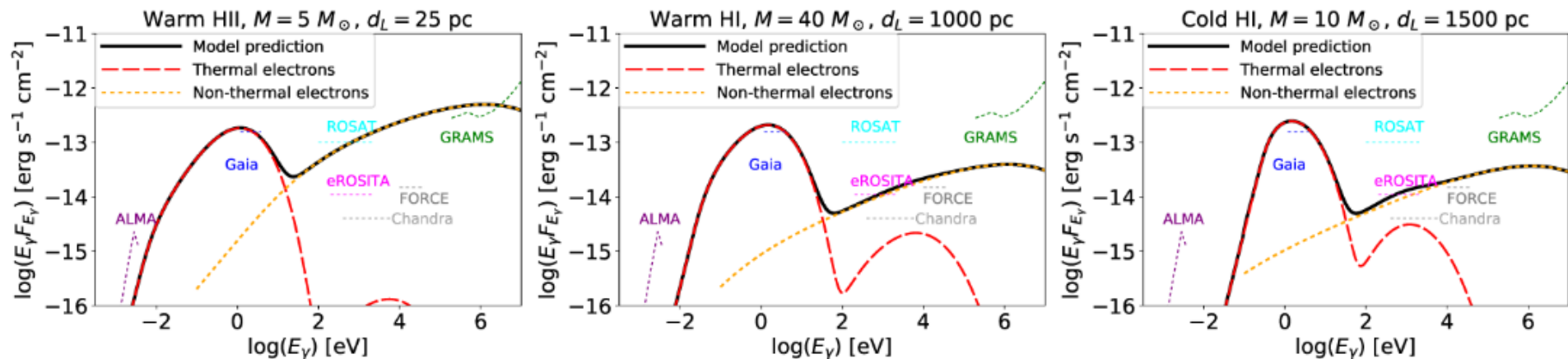
$$N_p \approx \frac{\dot{M}_\bullet}{4\pi R H V_R \mu_{\text{ISM}} m_p}$$

$$\simeq 2.3 \times 10^{10} \dot{M}_{\bullet,11} M_1^{-2} \mathcal{R}_1^{-3/2} \alpha_{-0.5}^{-1} \text{ cm}^{-3}$$

$$B = \sqrt{\frac{8\pi N_p k_B T_p}{\beta}}$$

$$\simeq 1.5 \times 10^4 \dot{M}_{\bullet,11}^{1/2} M_1^{-1} \mathcal{R}_1^{-5/4} \alpha_{-0.5}^{-1/2} \beta_{-1}^{-1/2} \text{ G},$$

MADs are expected to be formed when the mass accretion rate onto the BH is significantly lower than the Eddington rate.



Role of ionization due to accretion luminosity

$$\dot{M}_{\text{PR13}} = 4\pi \frac{(GM)^2 \rho_{\text{in}}}{(v_{\text{in}}^2 + c_{s,\text{in}}^2)^{3/2}}$$

$$\rho_{\text{in}} v_{\text{in}} = \rho v_{\text{BH}} ,$$

$$\rho_{\text{in}} (v_{\text{in}}^2 + c_{s,\text{in}}^2) = \rho (v_{\text{BH}}^2 + c_s^2)$$

$$\rho_{\text{in}} = \rho_{\text{in}}^{\pm} \equiv \rho \frac{v_{\text{BH}}^2 + c_s^2 \pm \sqrt{\Delta}}{2c_{s,\text{in}}^2} , \quad \Delta \equiv (v_{\text{BH}}^2 + c_s^2)^2 - 4v_{\text{BH}}^2 c_{s,\text{in}}^2$$

$$v_{\text{in}} = \frac{\rho}{\rho_{\text{in}}} v_{\text{BH}} ,$$

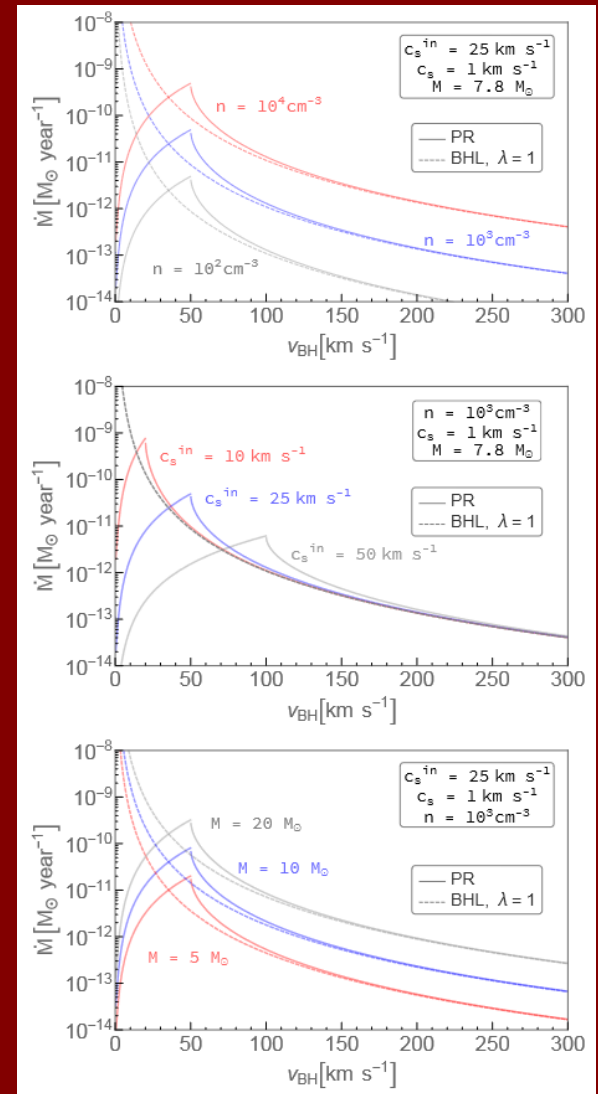
$$v_{\text{R}} \approx 2c_{s,\text{in}} ,$$

$$v_{\text{D}} \approx \frac{c_s^2}{2c_{s,\text{in}}} \ll 1 \text{ km/s.}$$

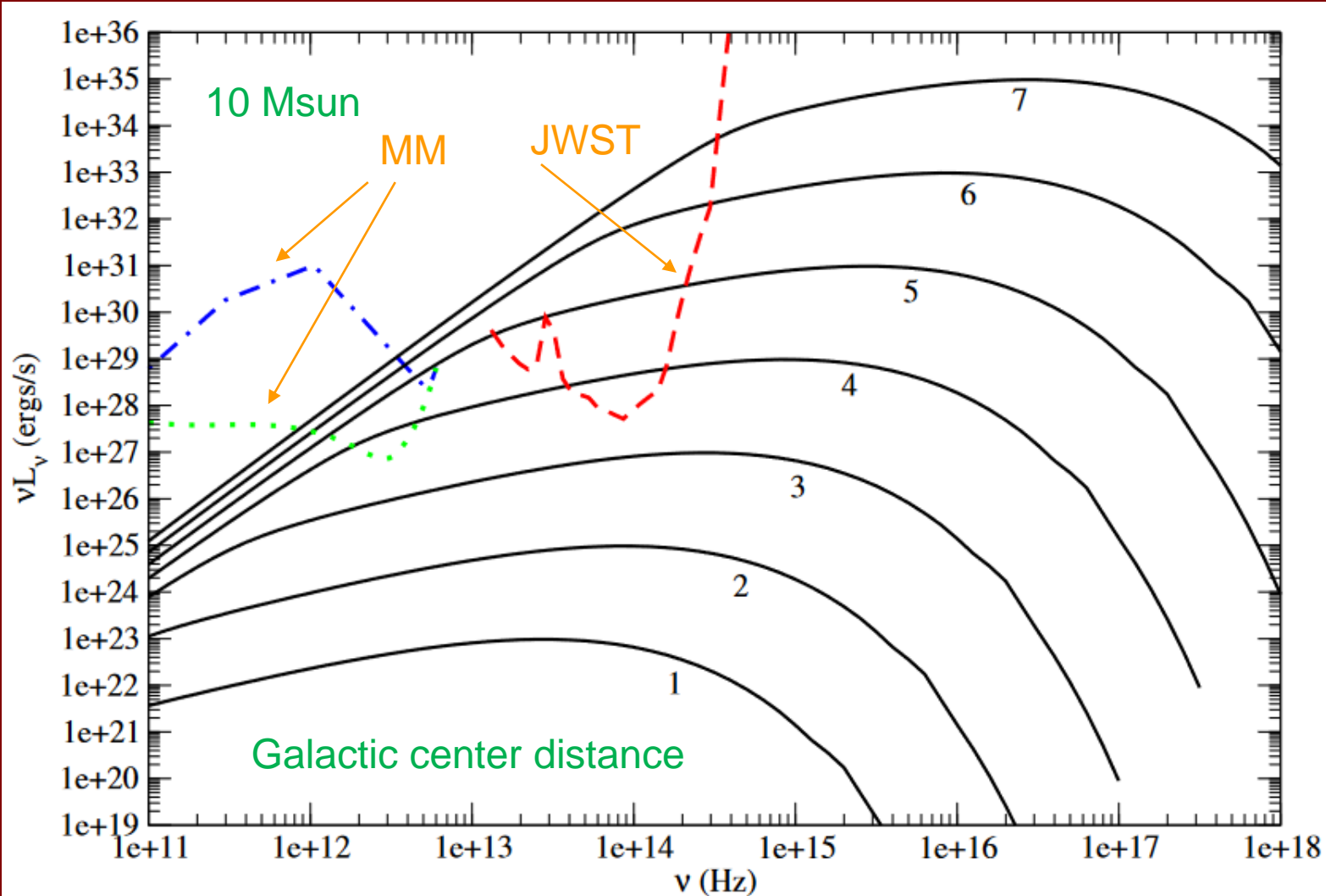
Roots of Delta.

For $v_{\text{D}} \leq v_{\text{BH}} \leq v_{\text{R}}$

$$\dot{M}_{\text{PR13}} = \pi \frac{(GM)^2 \rho (v_{\text{BH}}^2 + c_s^2)}{\sqrt{2} c_{s,\text{in}}^5}$$



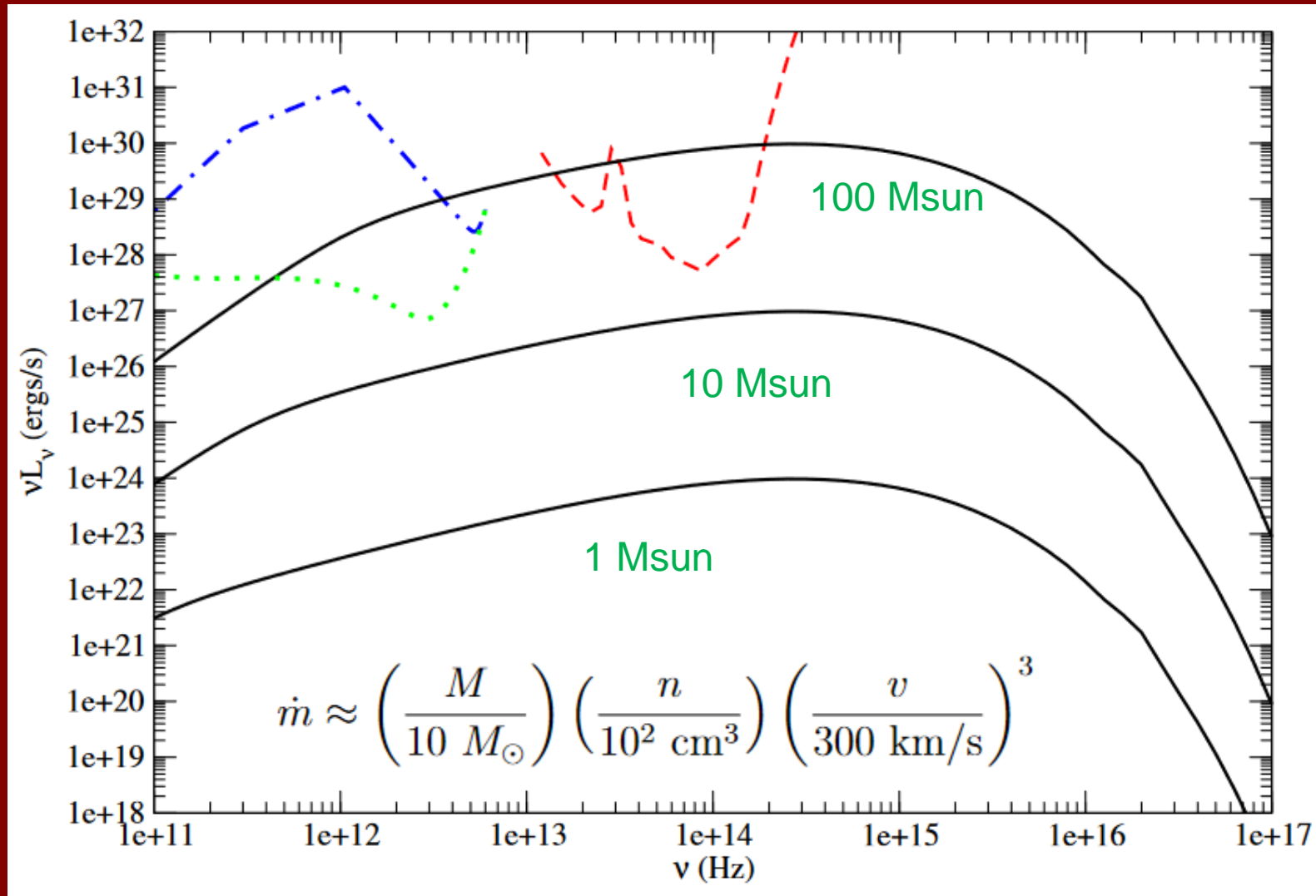
Perspectives for JWST and Millimetron



1905.04923

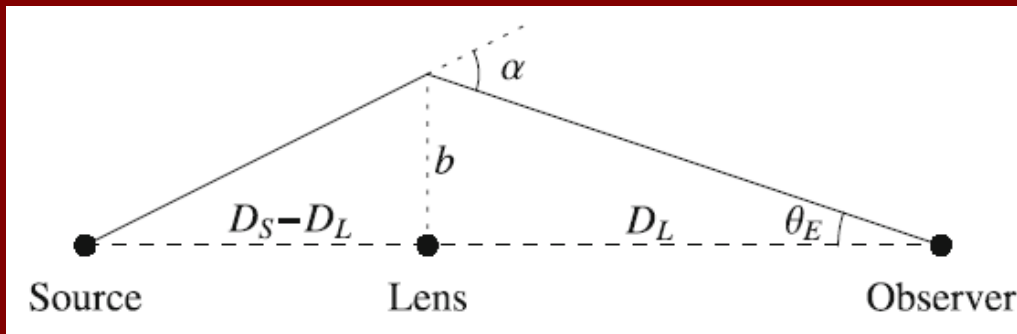
Different spectra are for different accretion rates:
from 10^{-10} up to 10^{-4} of Eddington

Orion cloud distance



1905.04923

Gravitational microlensing - 1



Probability of microlensing is small.
For stars it is $\sim 10^{-5} - 10^{-6}$ per year.

$$b = D_L \theta_E,$$

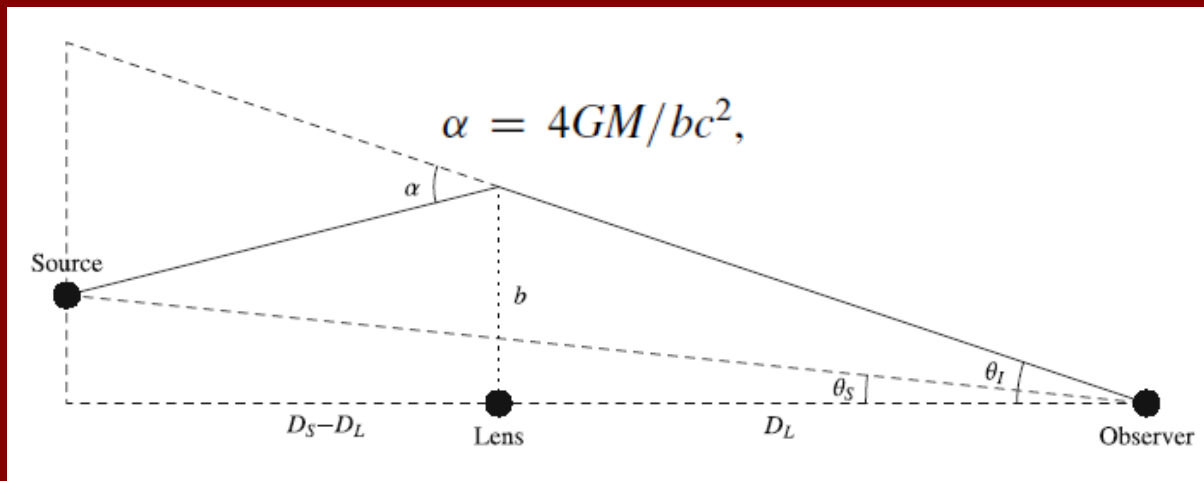
$$\alpha = b/D_L + b/(D_S - D_L).$$

$$\theta_E = \sqrt{\kappa M \pi_{\text{rel}}}; \quad \kappa \equiv \frac{4G}{c^2 \text{AU}} \simeq 8.14 \frac{\text{mas}}{M_\odot},$$

$$\pi_{\text{rel}} = \text{AU}(D_L^{-1} - D_S^{-1})$$

$$\tau = \int dD_L \pi (D_L \theta_E)^2 n(D_L) \sim \frac{4\pi G M n}{c^2} D^2 = \frac{4\pi G \rho}{c^2} D^2 \sim \frac{G M_{\text{tot}}}{D c^2} \sim \frac{v^2}{c^2}$$

Gravitational microlensing - 2



$$(\theta_I - \theta_S)D_S = \alpha(D_S - D_L)$$

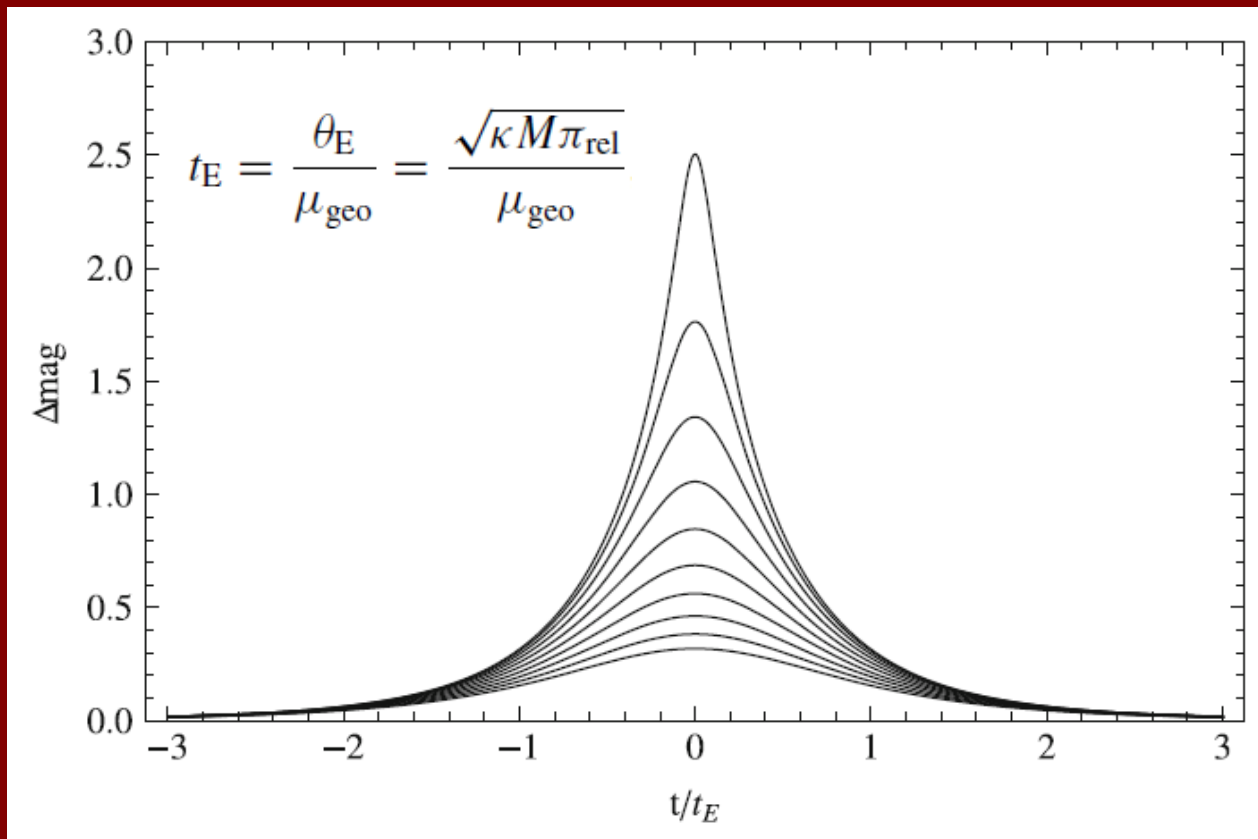
$$\theta_I(\theta_I - \theta_S) = \frac{4GM\pi_{\text{rel}}}{c^2 \text{AU}} \equiv \theta_E^2.$$

$$A_{\pm} = \pm \frac{u_{\pm}}{u} \frac{\partial u_{\pm}}{\partial u} = \frac{A \pm 1}{2}$$

$$u_{\pm} = \frac{u \pm \sqrt{u^2 + 4}}{2}; \quad u \equiv \frac{\theta_S}{\theta_E} \quad u_{\pm} \equiv \frac{\theta_{I,\pm}}{\theta_E}.$$

$$A = \frac{u^2 + 2}{u\sqrt{u^2 + 4}} = (1 - Q^{-2})^{-1/2}; \quad Q \equiv 1 + \frac{u^2}{2},$$

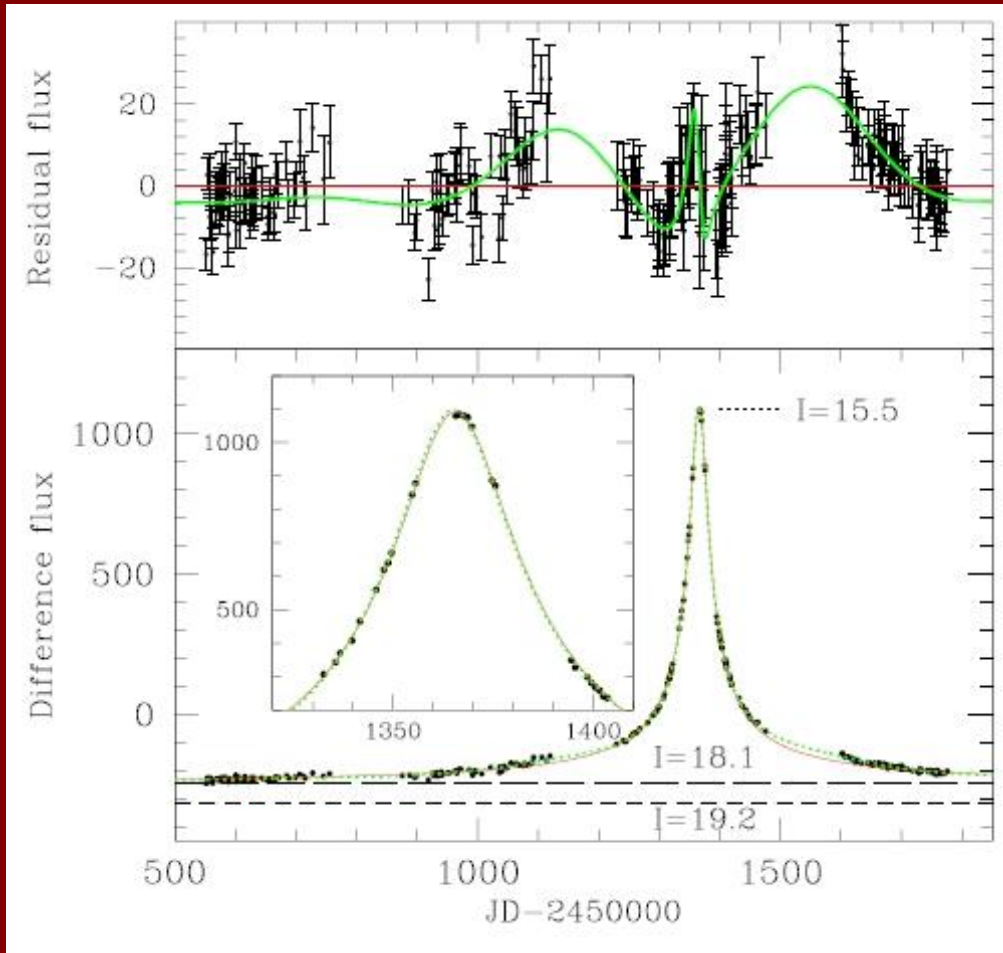
Light curves for point lenses



$$F(t) = f_s A(\mathbf{u}(t; t_0, u_0, t_E), \rho) + f_b;$$

$$\mathbf{u}(t; t_0, u_0, t_E) = (\tau(t), \beta) = \left(\frac{t - t_0}{t_E}, u_0 \right).$$

Microlensing and isolated BHs

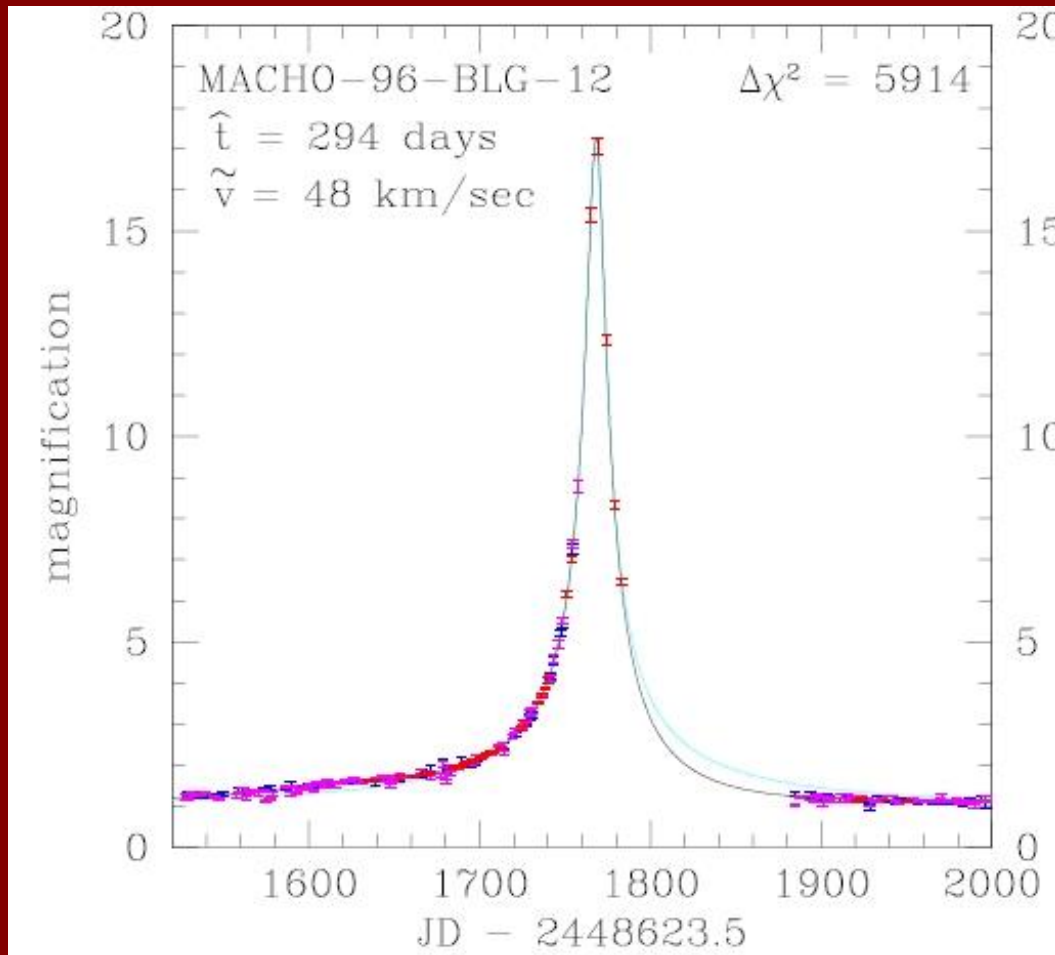


Event OGLE-1999-BUL-32

A very long event: 641 days.

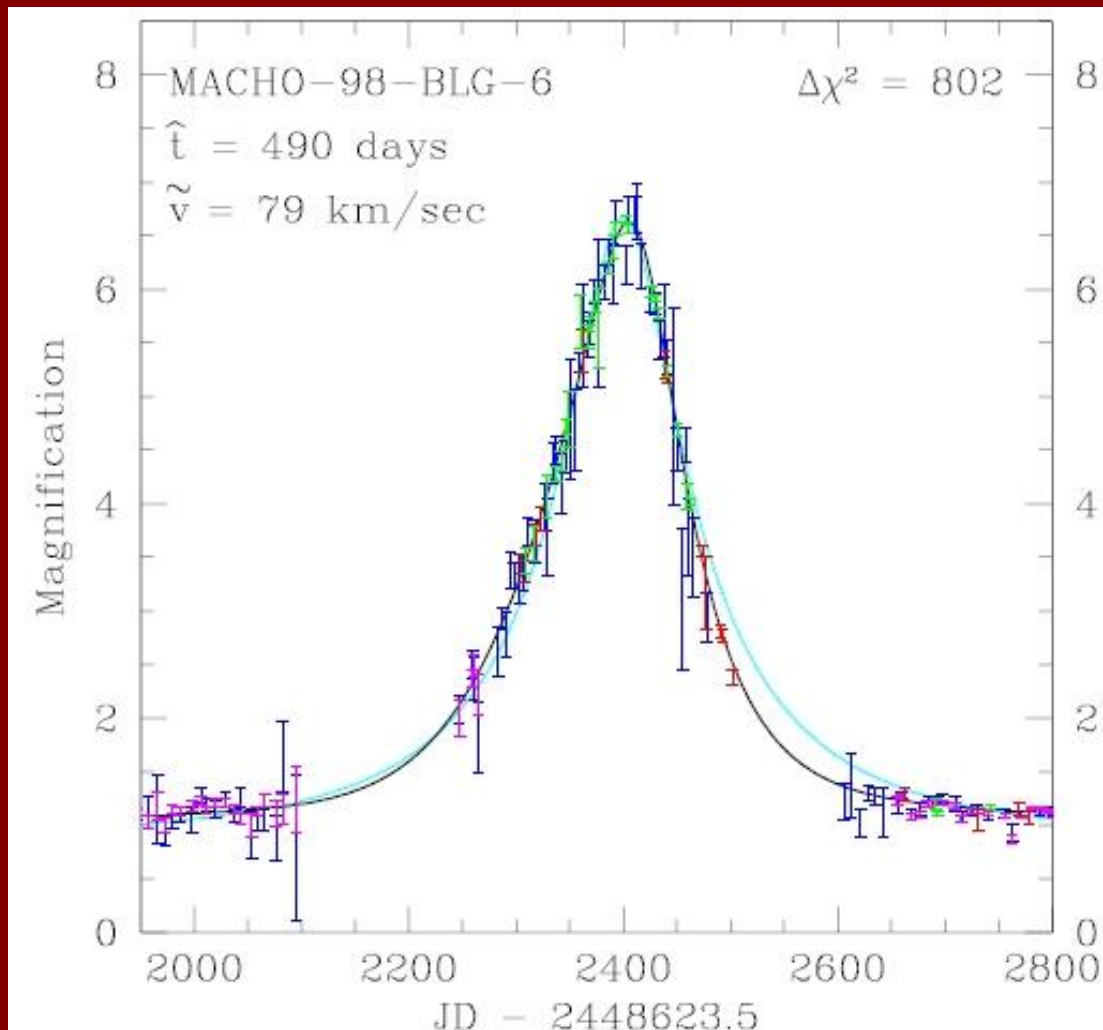
Mass estimate for the lense $>4 M_0$

Microlensing – the MACHO project



MACHO-96-BLG-6
3-16 solar masses.

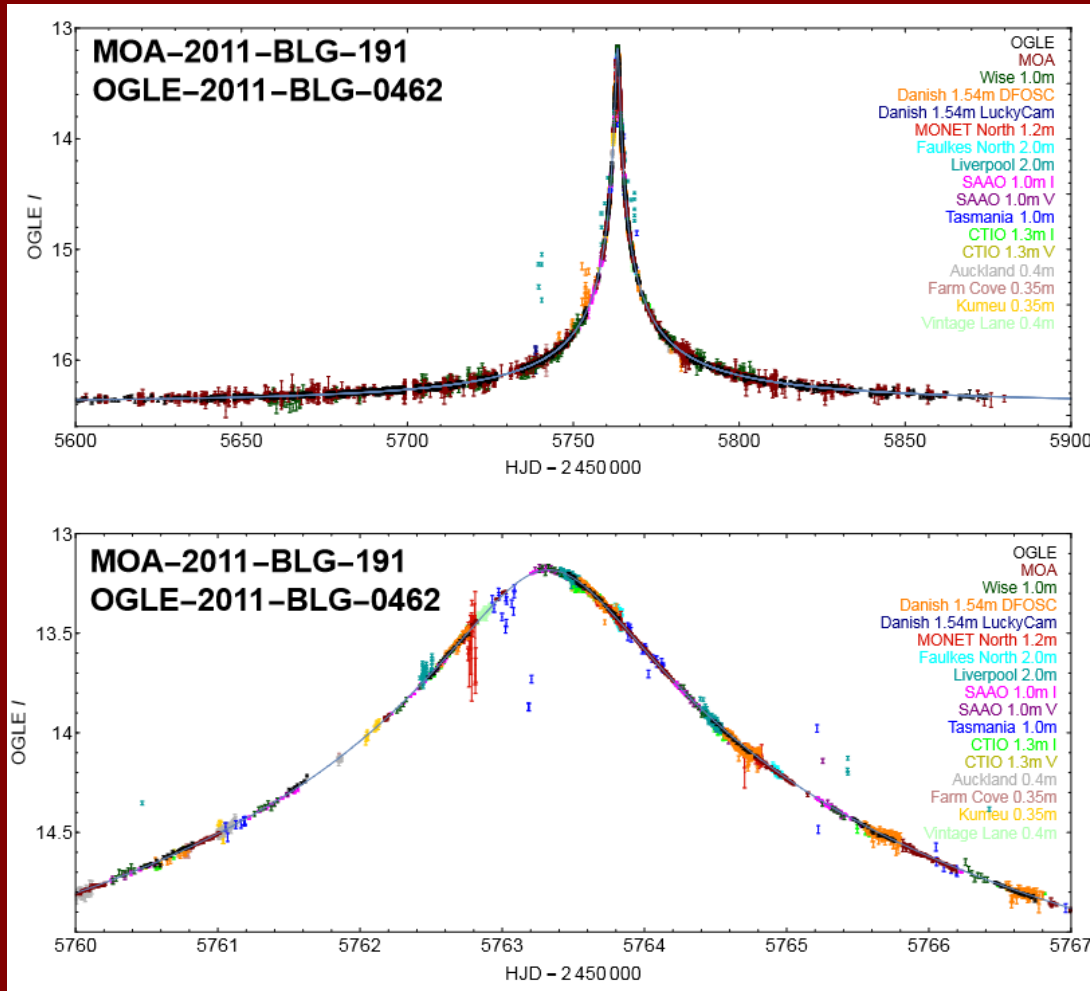
Again MACHO!



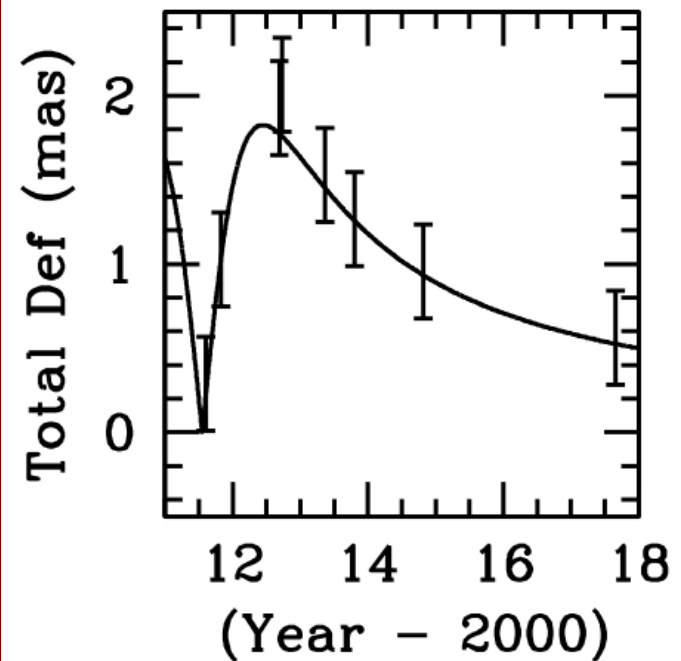
MACHO-98-BLG-6
3-13 solar masses.

Photometric + astrometric = The Best

MOA-2011-BLG-191/OGLE-2011-BLG-0462. $M=1.6\text{--}4.2$ Msolar



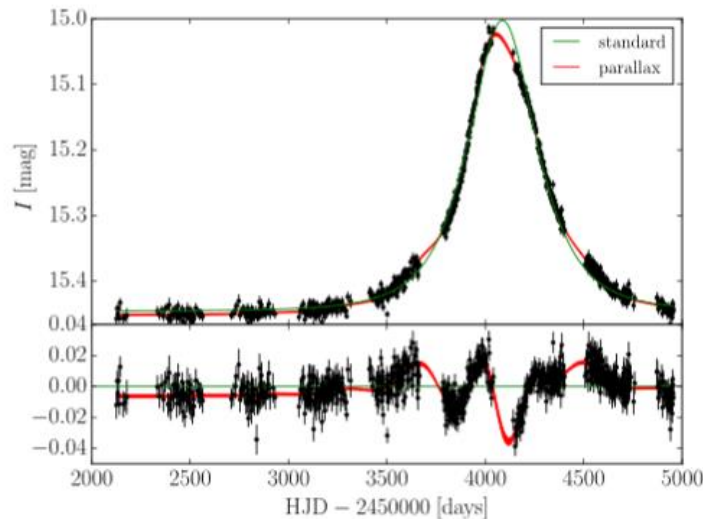
This is the first case when both – photometric and astrometric, - lensing is observed for a BH lense.



2202.01903, 2201.13296

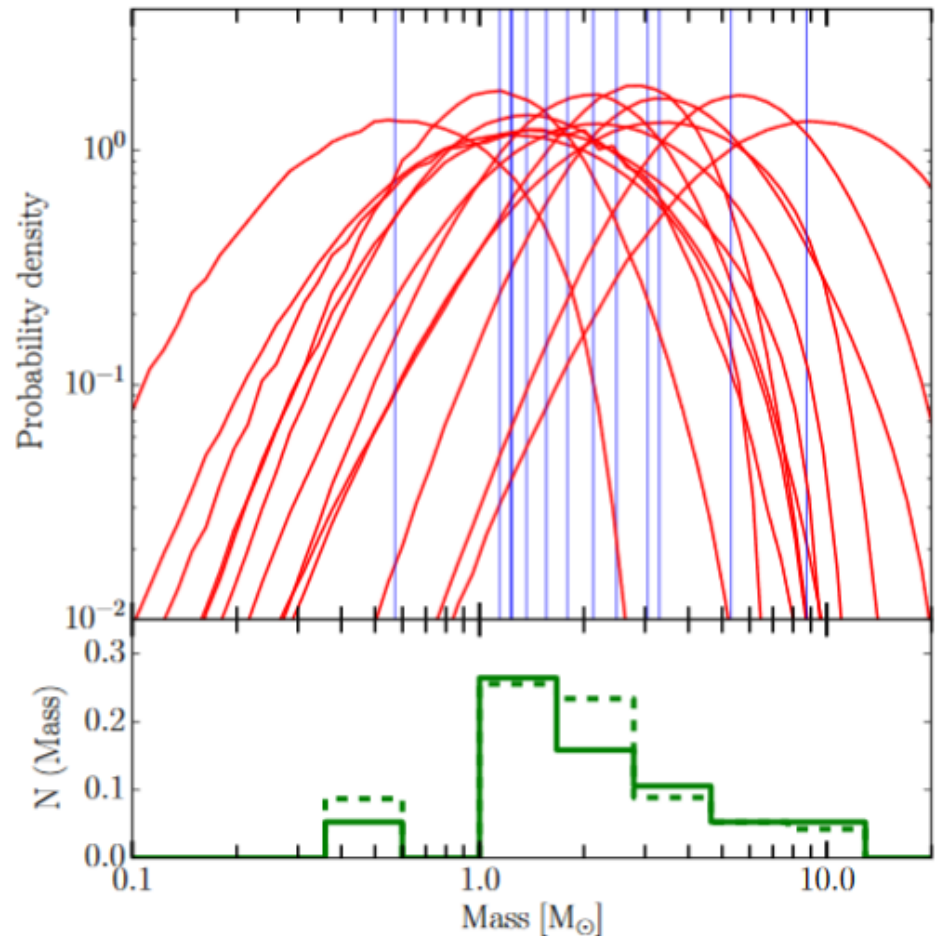
More examples

OGLE-III data



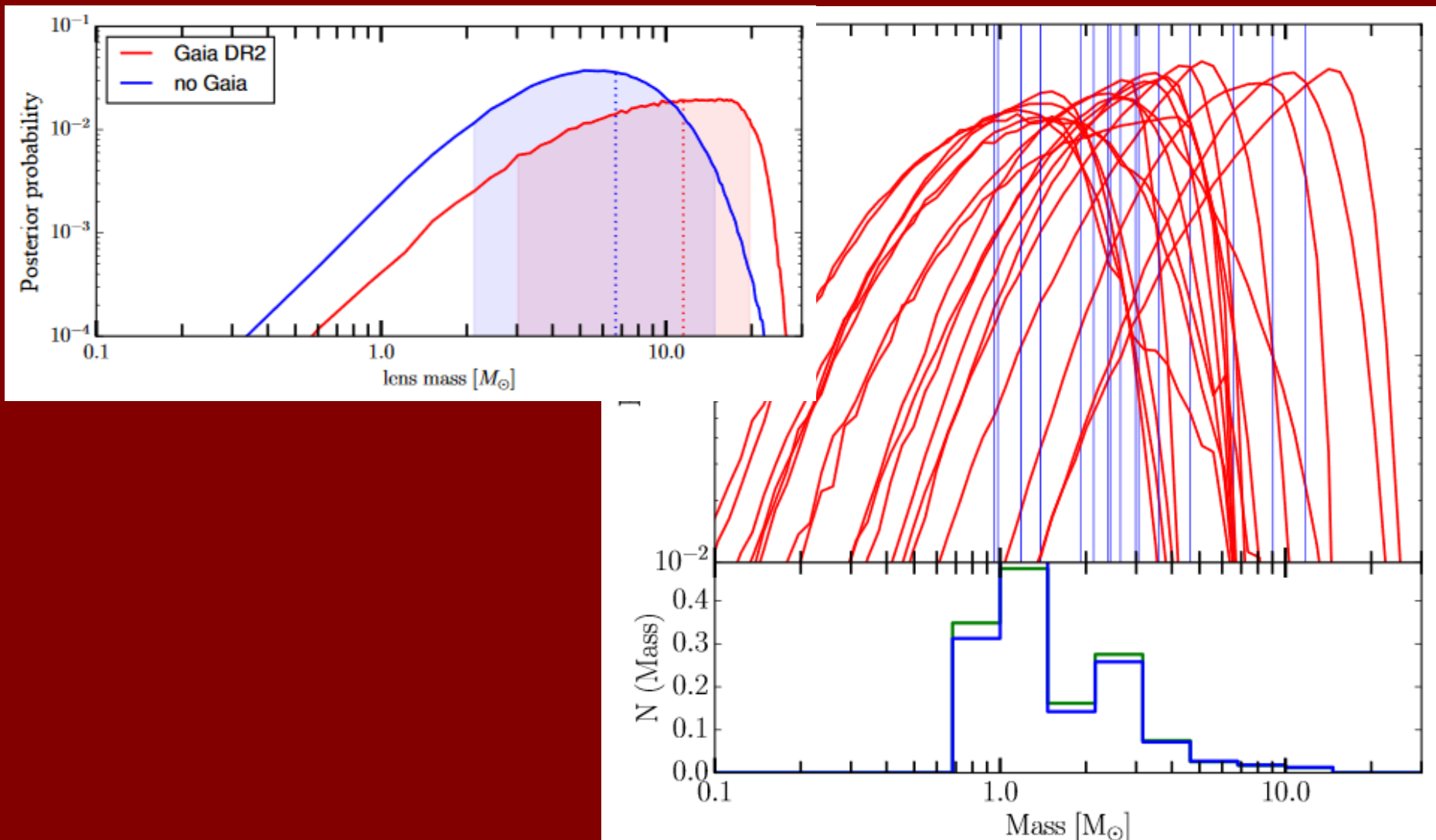
OGLE3-ULENS-PAR-02
8.7 solar masses at 1.8 kpc

Altogether 13 candidates
for WD, NS, or BH lensing.

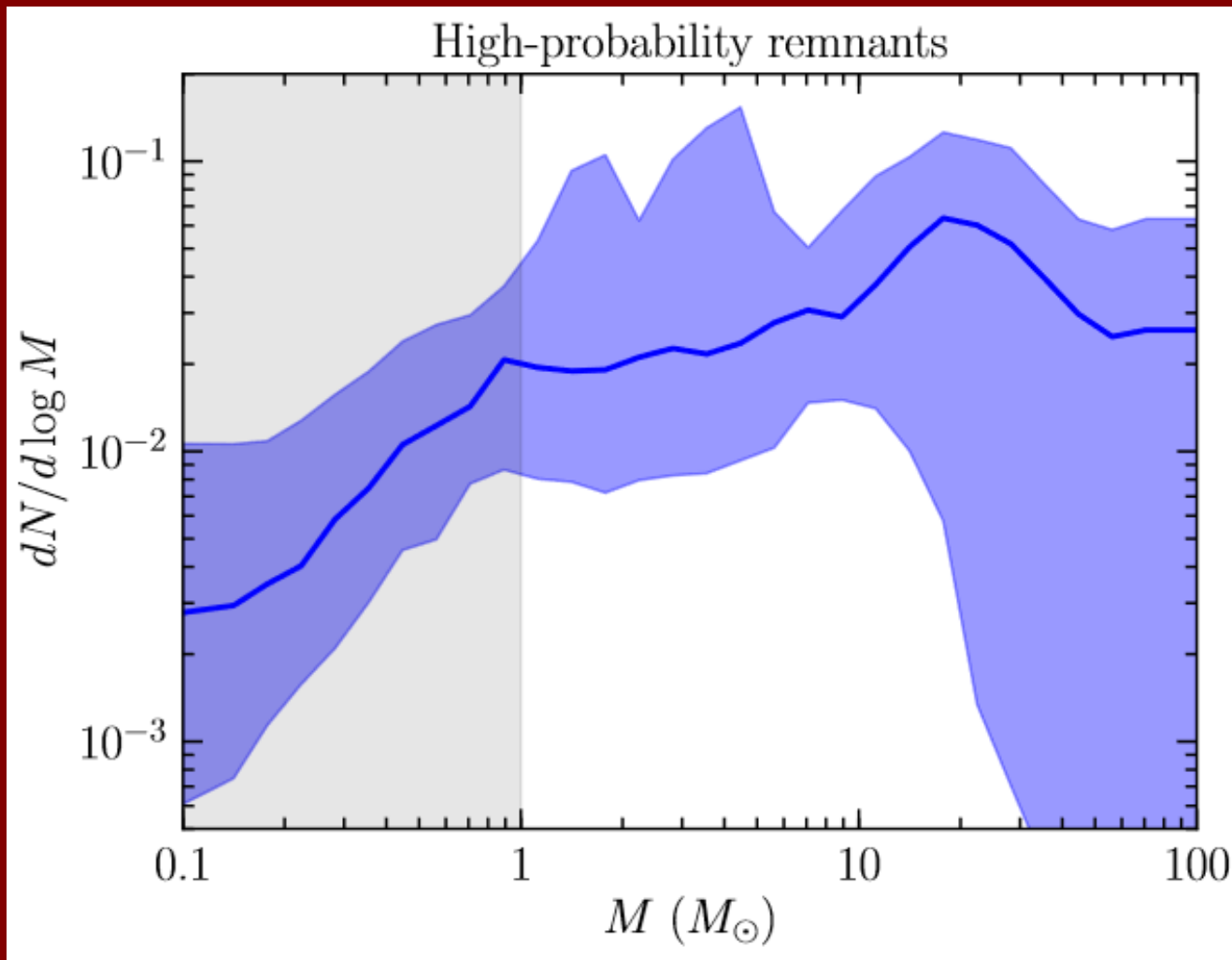


1509.04899, see also 1601.02830

Gaia helps to estimate mass of lenses

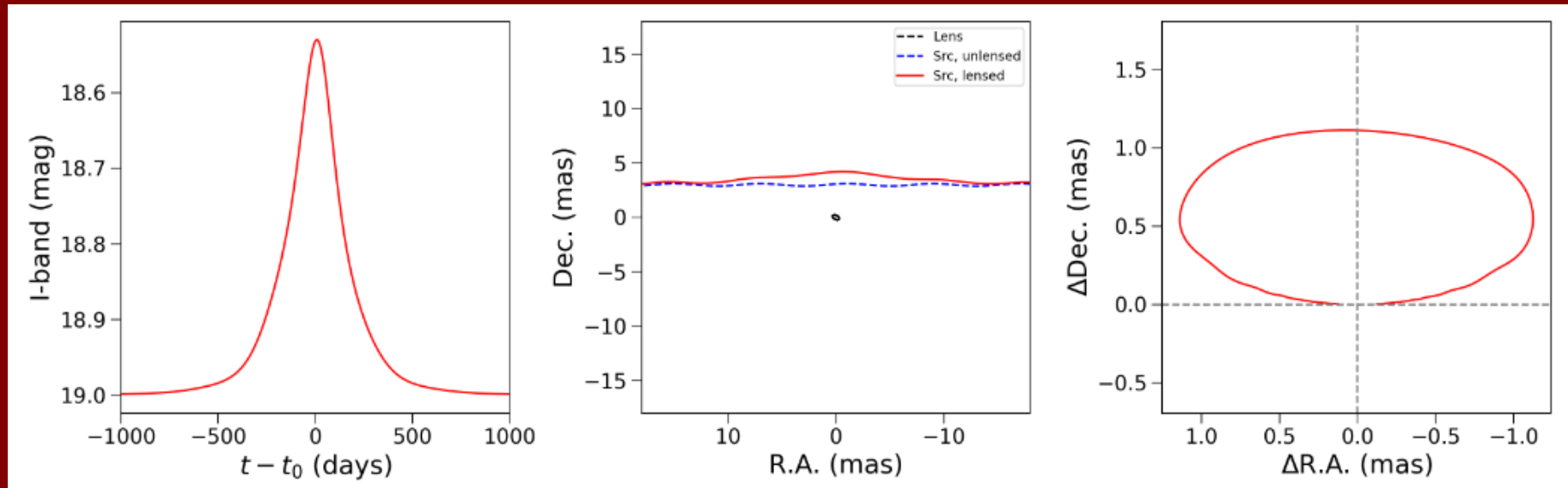


Mass function basing on OGLE-III



Selection effects are very important.

Photometric and astrometric



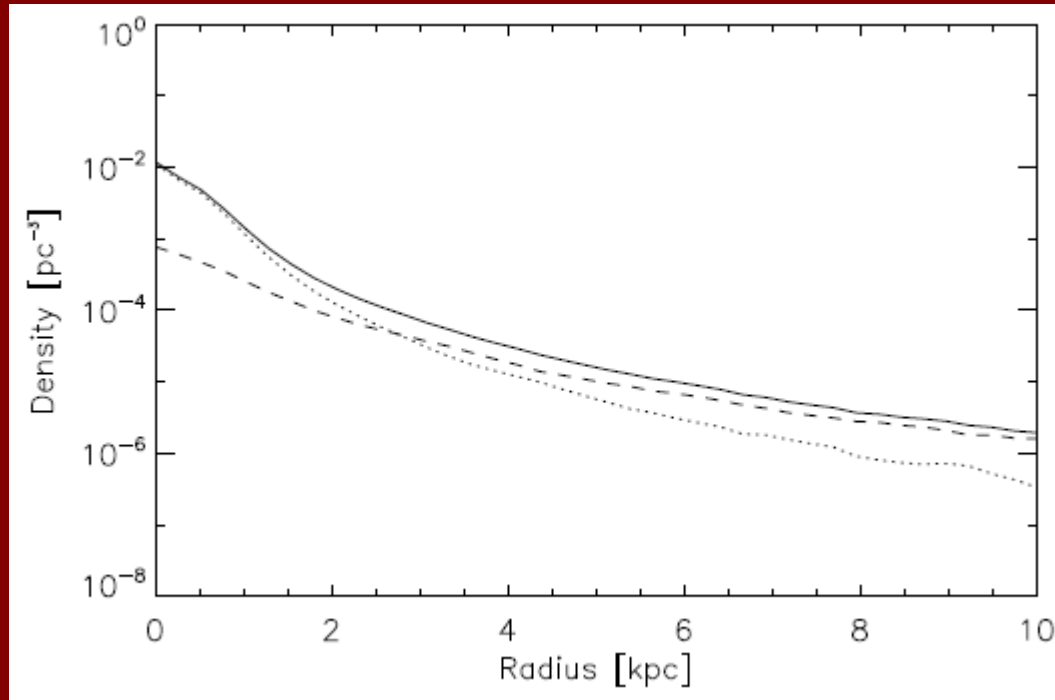
Photometry and astrometry for a black hole at 3 kpc
lensing a background star at 6 kpc with a relative proper motion of 8 mas yr^{-1} .

Left: Photometric light-curve.

Center: Astrometry of the lens and source, with parallax, as would be seen on the sky.

Right: Astrometry of the lensed source after the proper motion is removed.

Probabilities of lensing

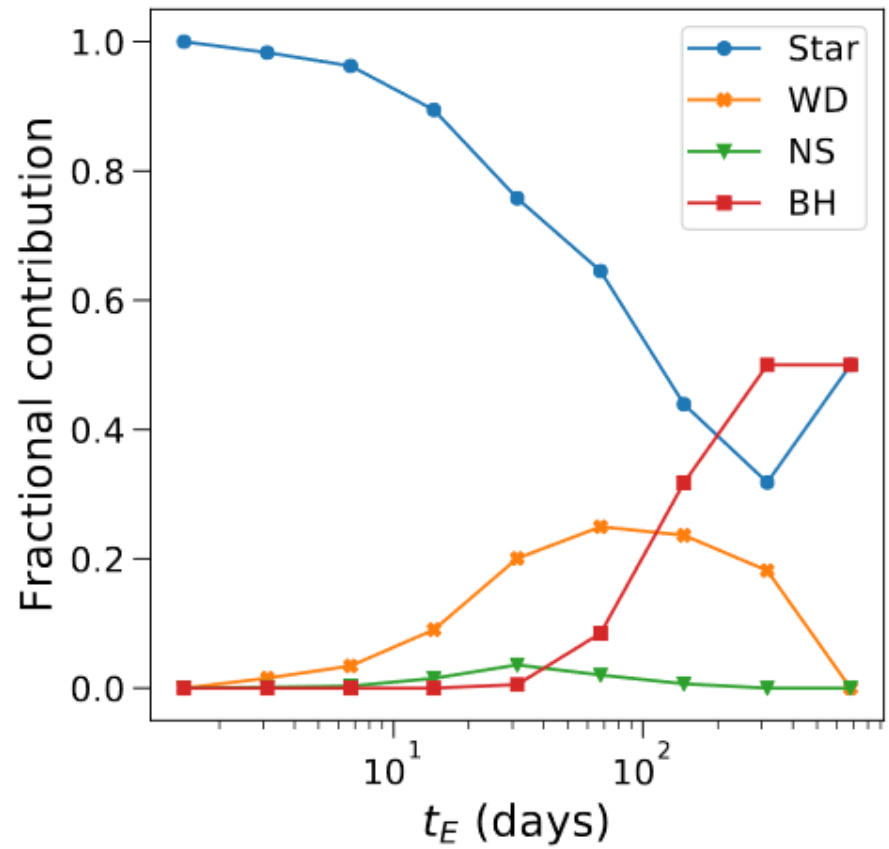
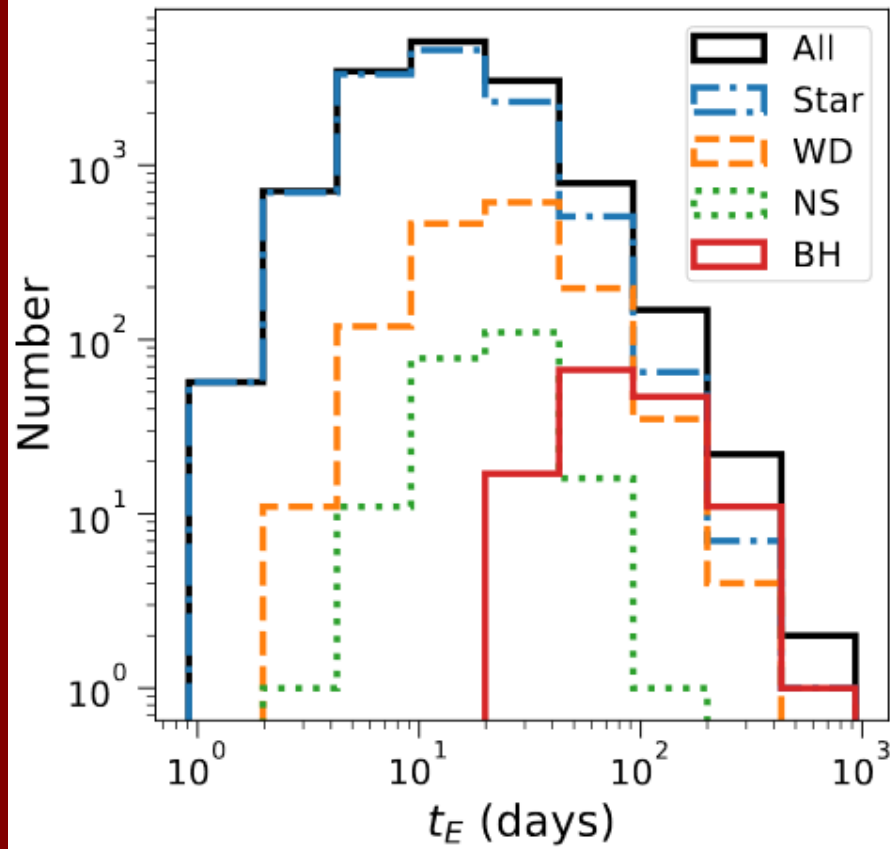


30-40% of events with >100 days are due to black holes

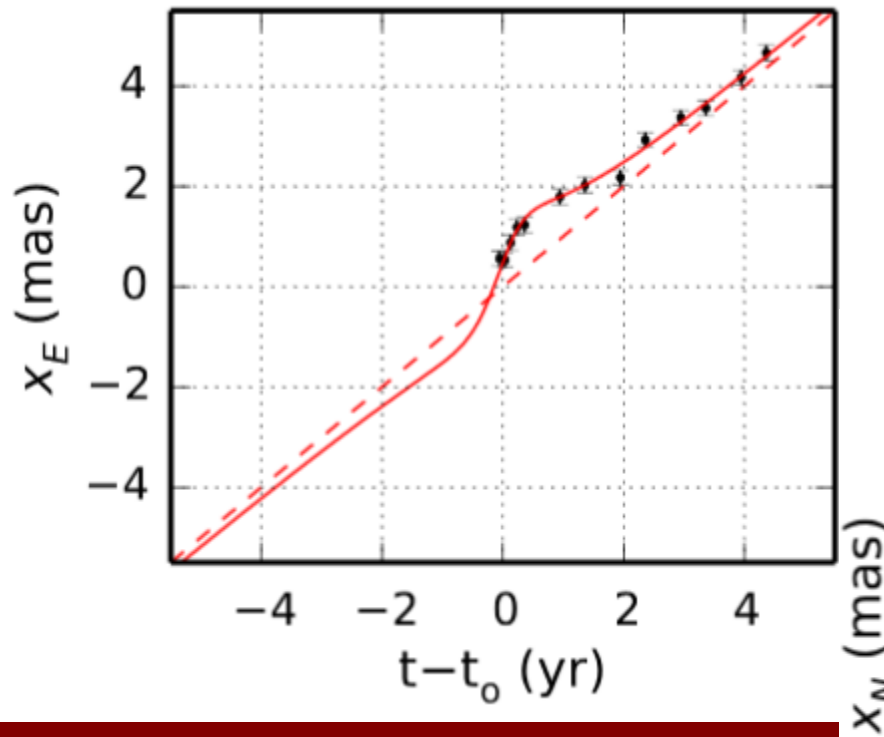
l.o.s. (l, b)	Γ_{star} [10^{-5} star $^{-1}$ yr $^{-1}$]	$\langle t_E \rangle_{star}$ [days]	Γ_{NS} [10^{-6} star $^{-1}$ yr $^{-1}$]	$\langle t_E \rangle_{NS}$ [days]	Γ_{BH} [10^{-6} star $^{-1}$ yr $^{-1}$]	$\langle t_E \rangle_{BH}$ [days]
($0^\circ, 0^\circ$)	2.67	16	1.47	25	0.38	67
($1^\circ, -3^\circ.9$)	0.52	20	0.40	28	0.10	77

Population synthesis of isolated BHs and NSs to predict microlensing events

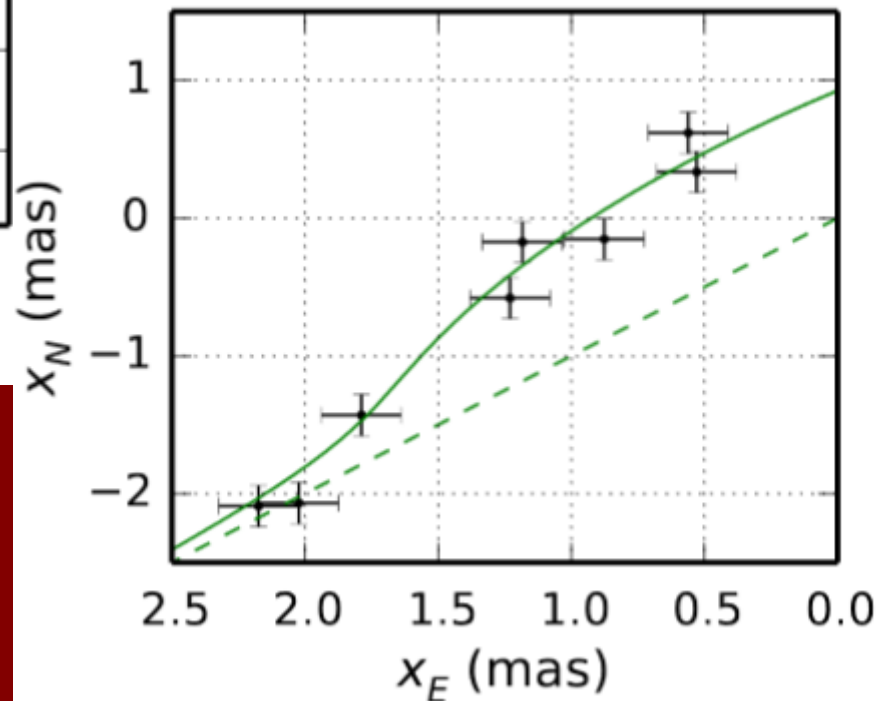
PooSvCLE:



Astrometric microlensing and BHs



A simulation of the 2D astrometric shift due a 10 solar masses BH at 4 kpc microlensing a background source at 8 kpc with a relative proper motion of 7 mas/yr and impact parameter $u_0=0.5$.

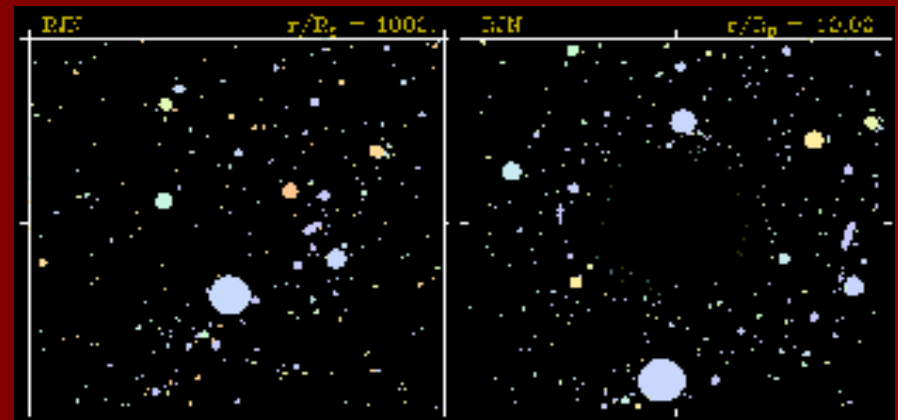


Also Gaia can contribute.

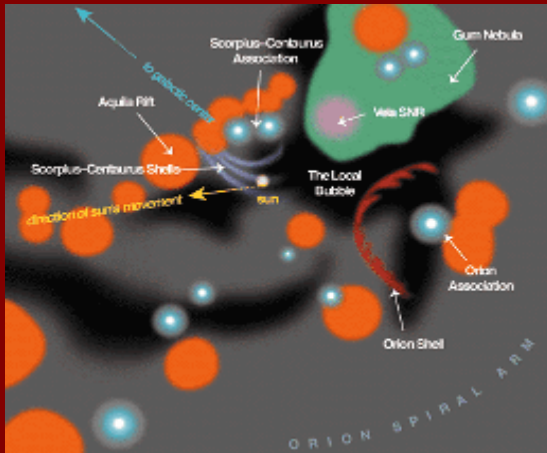
Black holes around us

- Black holes are formed from very massive stars
- It is very difficult to see an isolated black hole:
 - Microlensing
 - Accretion
 -?
- It is very important to have even a very approximate idea where to search. Let us look at our neighbourhood....

There should be about several tens of million isolated BHs in the Galaxy



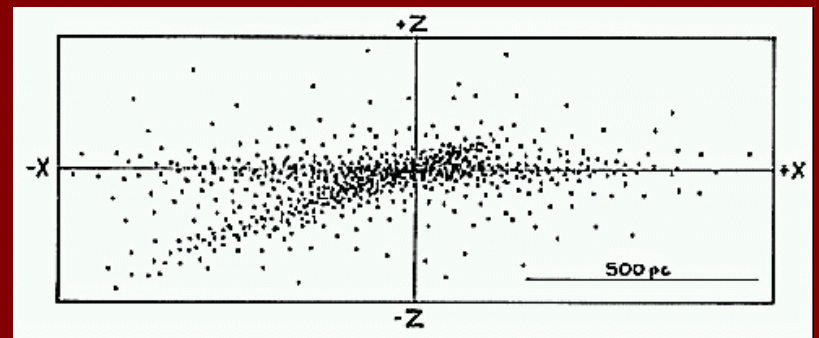
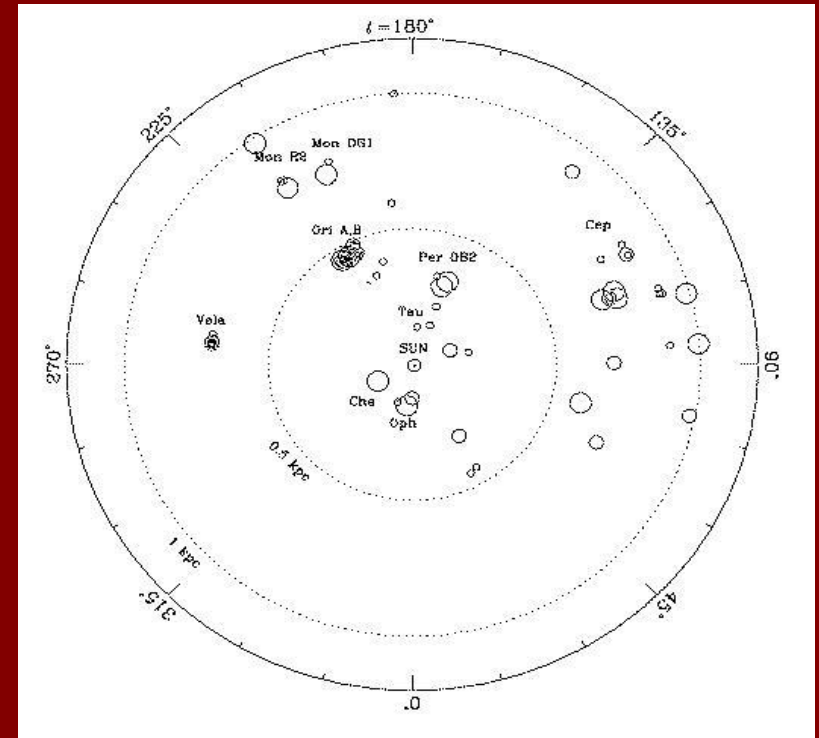
The Solar proximity



- The solar vicinity is not just an average “standard” region
- The Gould Belt
- $R=300\text{-}500$ pc
- Age: 30-50 mill. years
- 20-30 SN in a Myr (Grenier 2000)
- The Local Bubble
- Up 6 SN in several Myrs

The Gould Belt

- Poppel (1997)
- $R=300 - 500$ pc
- The age is about 30-50 million years
- A disc-like structure with a center 100-150 pc from the Sun
- Inclined respect to the galactic plane by $\sim 20^\circ$
- 2/3 of massive stars in 600 pc from the Sun belong to the Belt

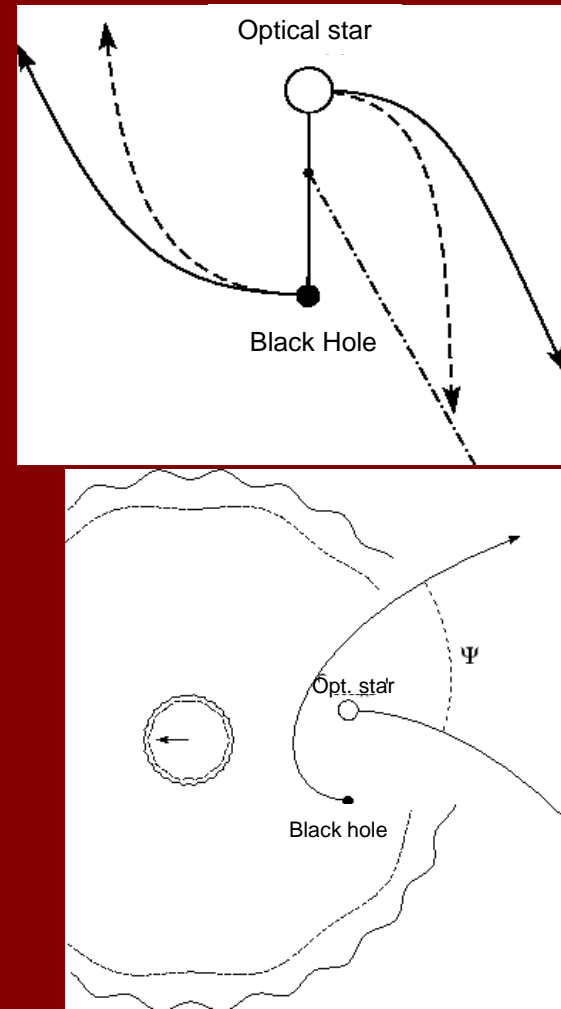
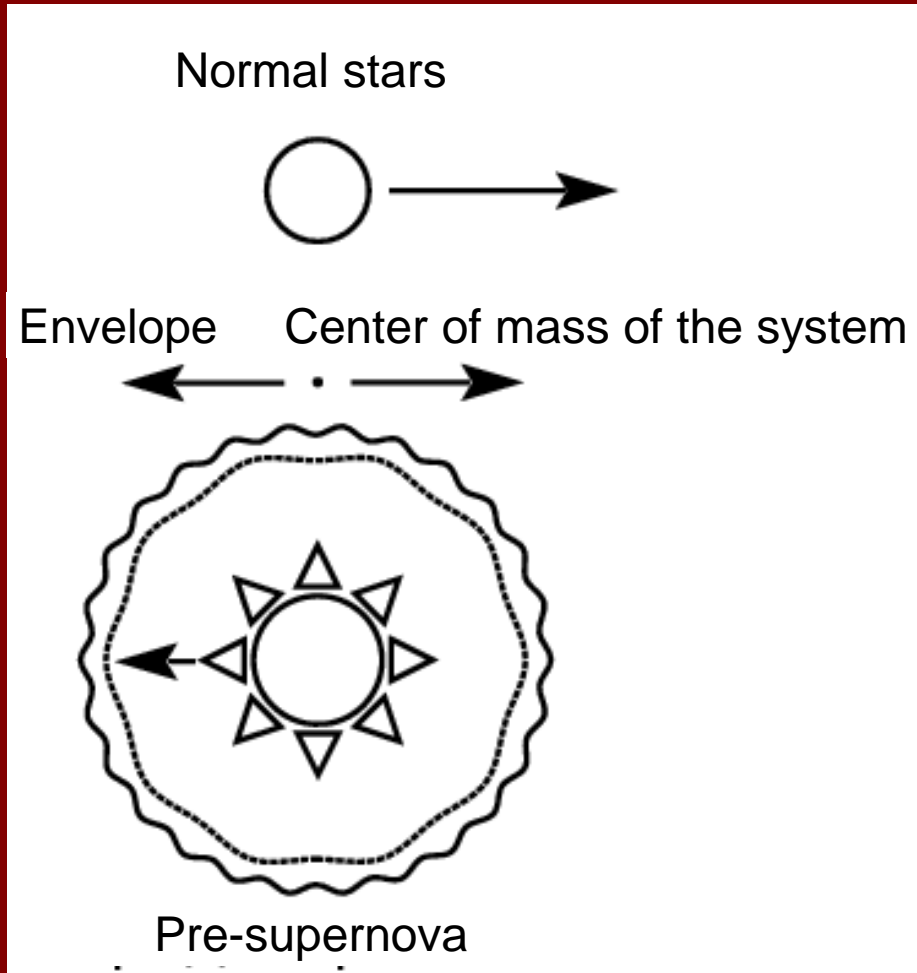


Close-by BHs and runaway stars

- 56 runaway stars inside 750 pc (Hoogerwerf et al. 2001)
- Four of them have $M > 30 M_{\text{solar}}$

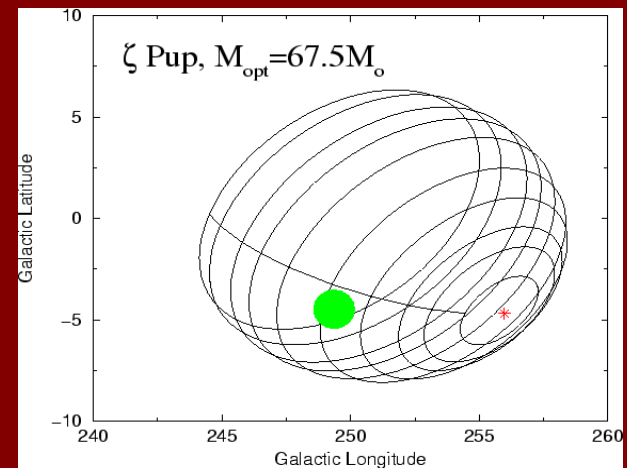
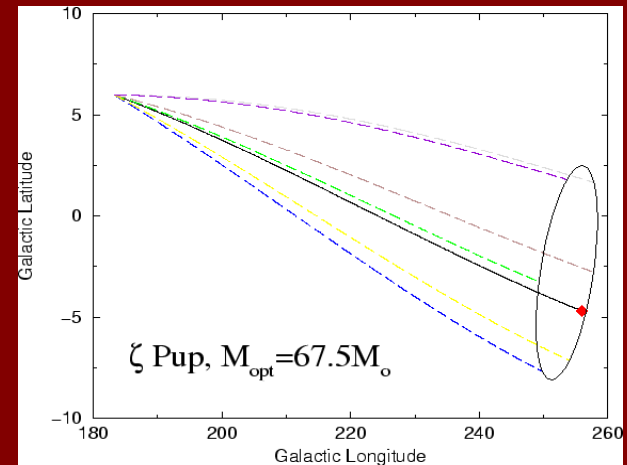
Star	Mass	Velocity km/s	Age, Myr
ξ Per	33	65	1
HD 64760	25-35	31	6
ς Pup	67	62	2
λ Cep	40-65	74	4.5

SN explosion in a binary



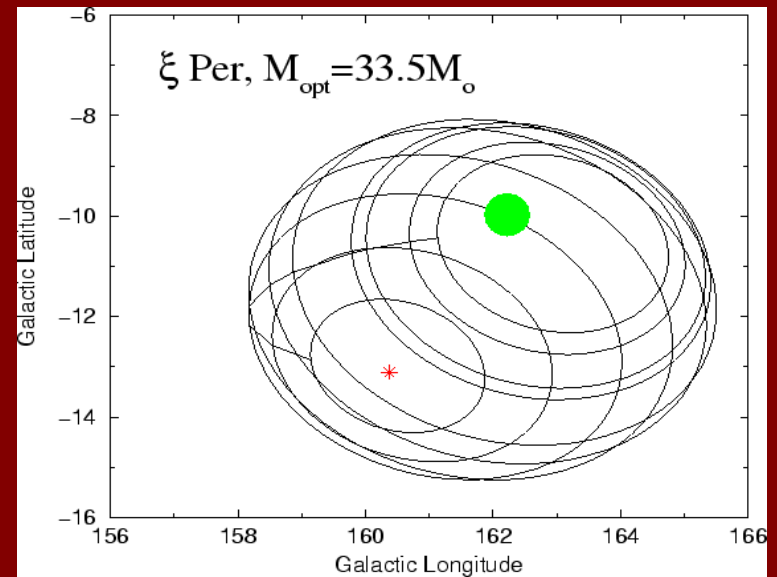
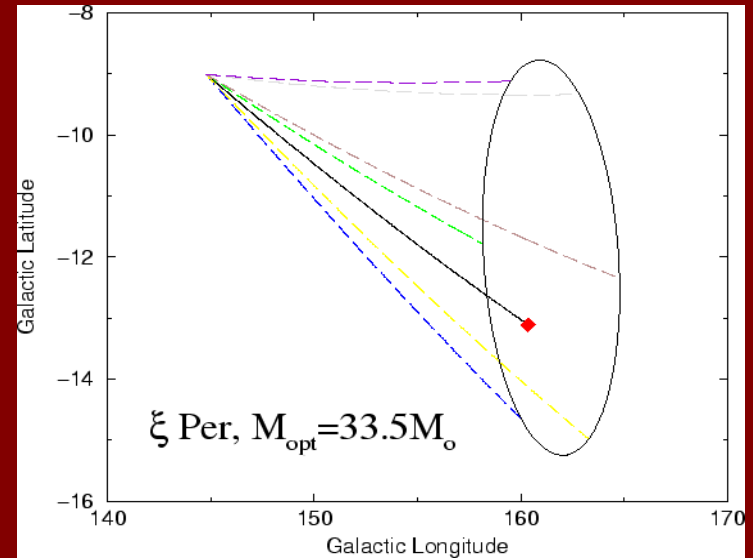
ζ Pup

- Distance: 404-519 pc
- Velocity: 33-58 km/s
- Error box: $12^\circ \times 12^\circ$
- N_{EGRET} : 1

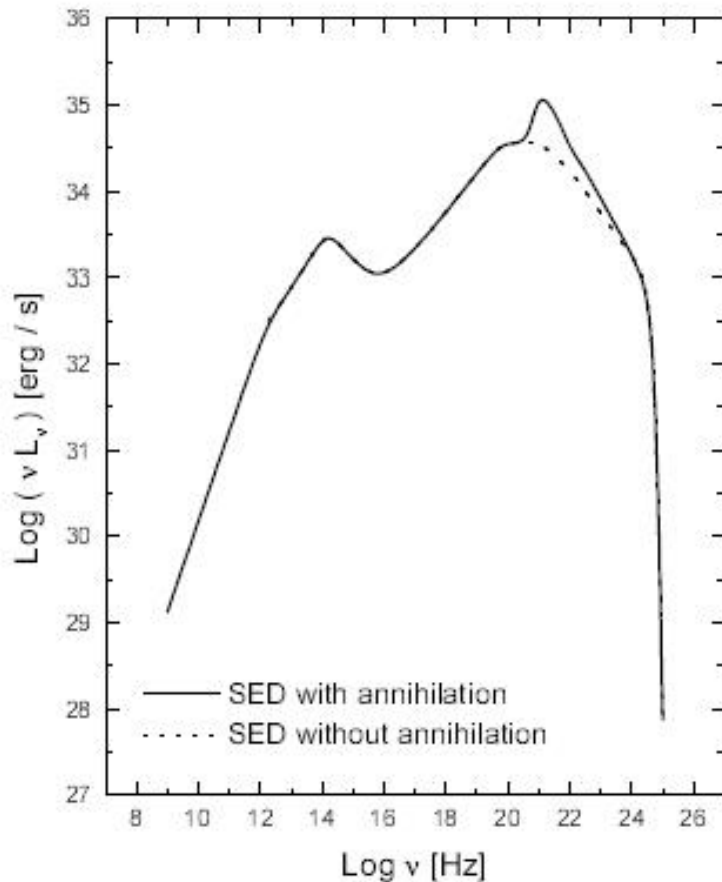


ξ Per

- Distance: 537-611 pc
- Velocity: 19-70 km/s
- Error box: $7^\circ \times 7^\circ$
- N_{EGRET} : 1



Gamma-ray emission from isolated BHs



Kerr-Newman isolated BH.

Magnetosphere. $B \sim 10^{11} \text{ G}$

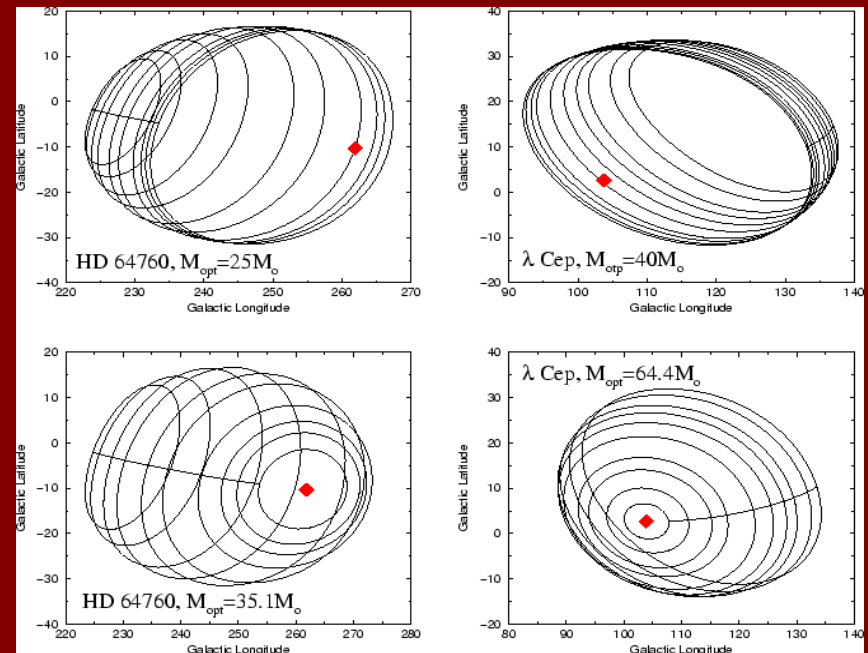
Jets.

See details about this theory
in Punsly 1998, 1999.

astro-ph/0007464, 0007465 – application to EGRET sources

Runaway BHs

- Approximate positions of young close-by BHs can be estimated basing on data on massive runaway stars
- For two cases we obtained relatively small error boxes
- For HD 64760 and for λ Cep we obtained very large error boxes (40-50°)
- Several EGRET sources inside



Resume

1. Accreting stellar mass isolated BHs
 - They should be! And the number is huge!
 - But sources are very weak.
 - Electron-positron jets and/or radio sources
 - Problems with identification, if there are no data in several wavelengths
2. Microlensing on isolated stellar mass BHs
 - There are several good candidates
 - But it is necessary to find the black hole ITSELF!
3. Exotic emission mechanisms
 - As all other exotics: interesting, but not very probable
 - If it works, then GLAST will show us isolated BHs
4. Runaway stars
 - A rare case to make even rough estimates of parameters
 - Error-boxes too large for any band except gamma-rays
 - All hope on the exotic mechanisms (Torres et al. astro-ph/0007465)